

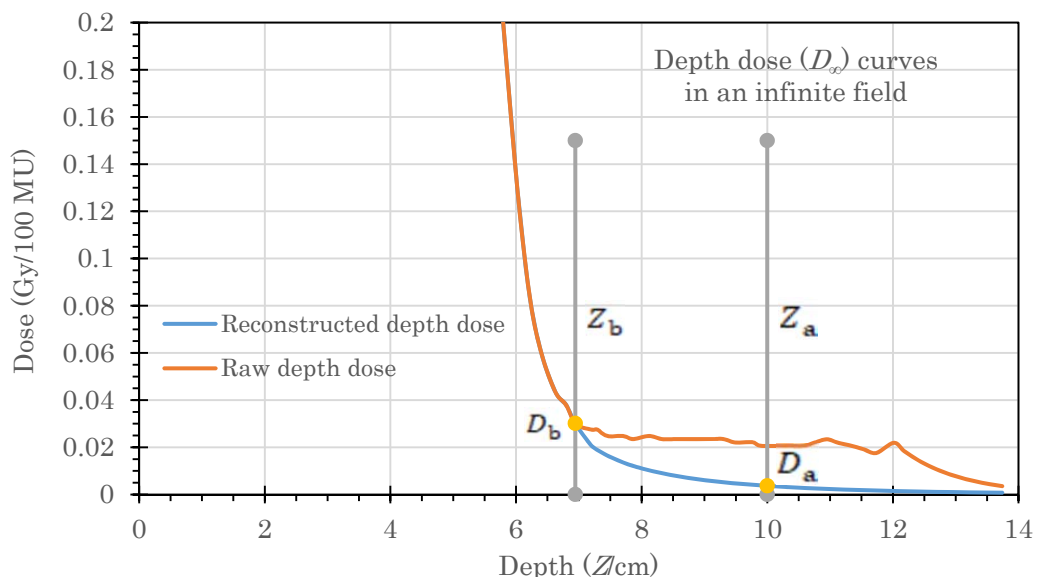
Supplementary material

Further development of the preceding Gaussian-pencil-beam-model used for calculation of the in-water dose caused by clinical electron-beam irradiation

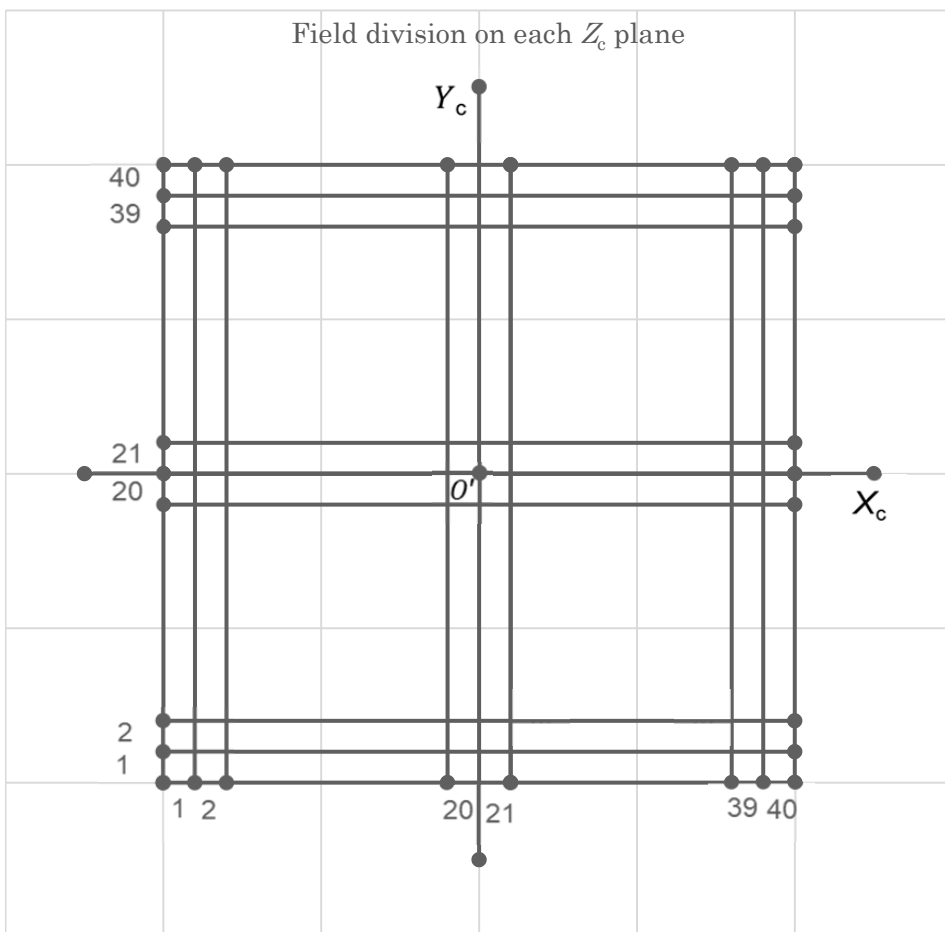
Akira Iwasaki, Shingo Terashima, Shigenobu Kimura, Kohji Sutoh, Kazuo Kamimura, Yoichiro Hosokawa, Masanori Miyazawa

<http://dx.doi.org/10.14312/2399-8172.2023-1>

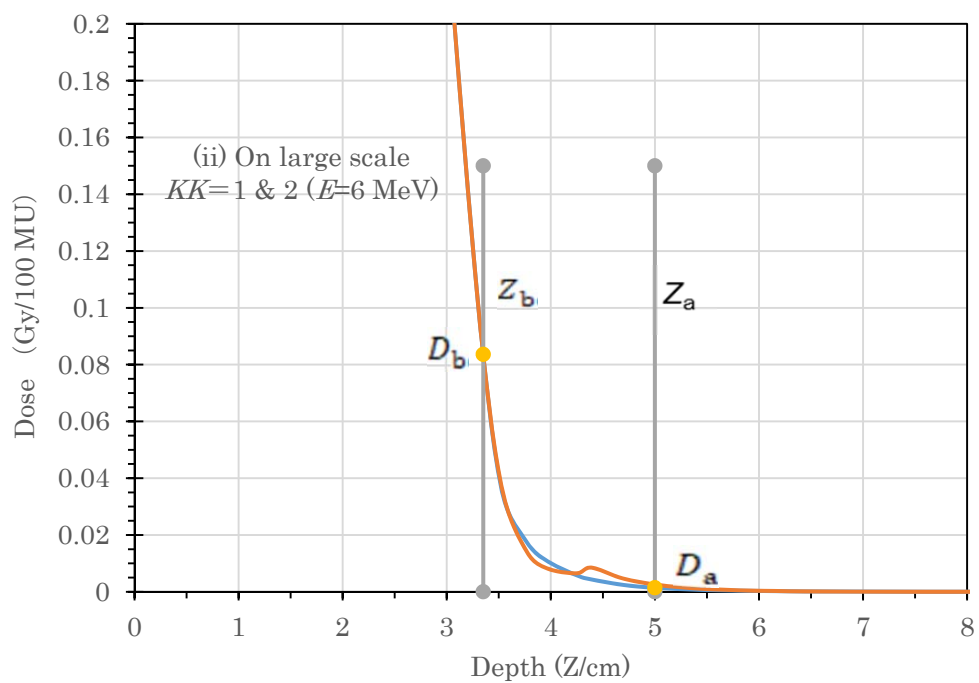
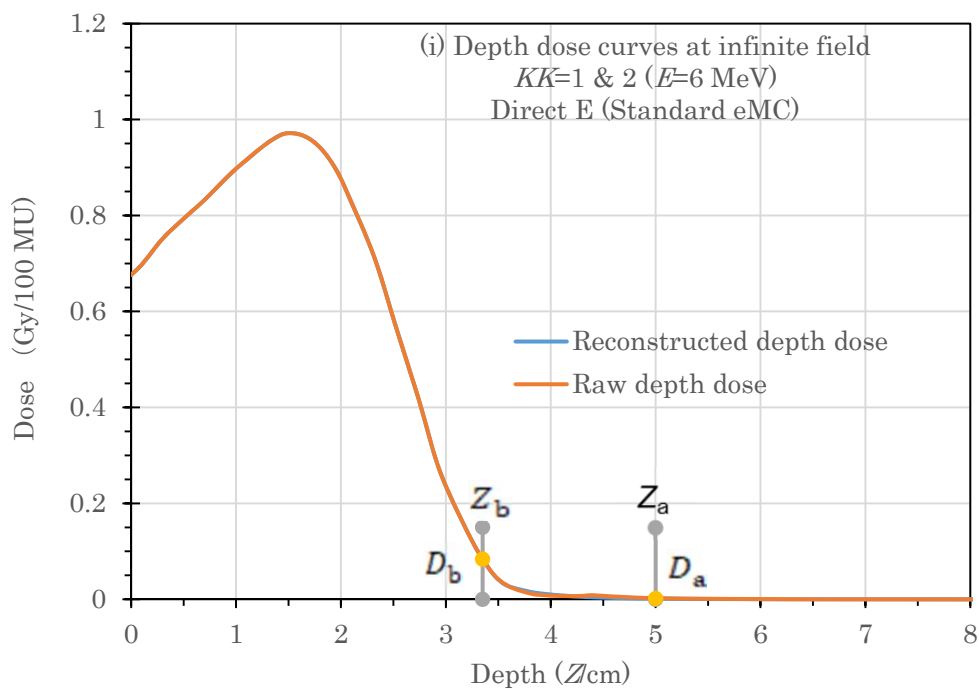
Supplementary Figures (Supp. Fig.)



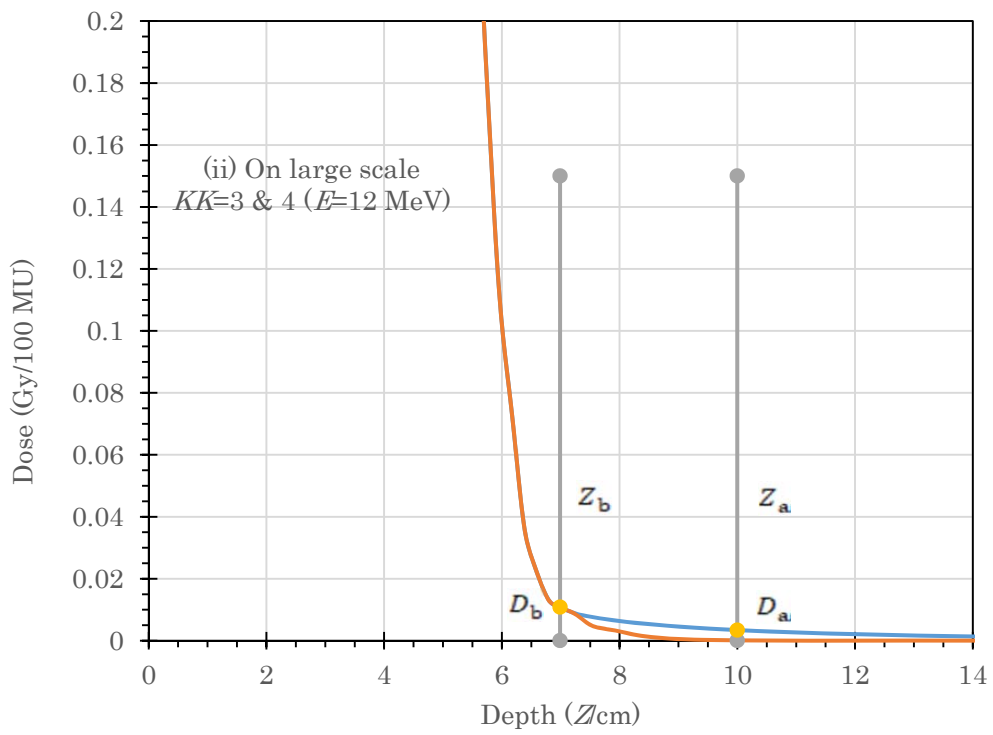
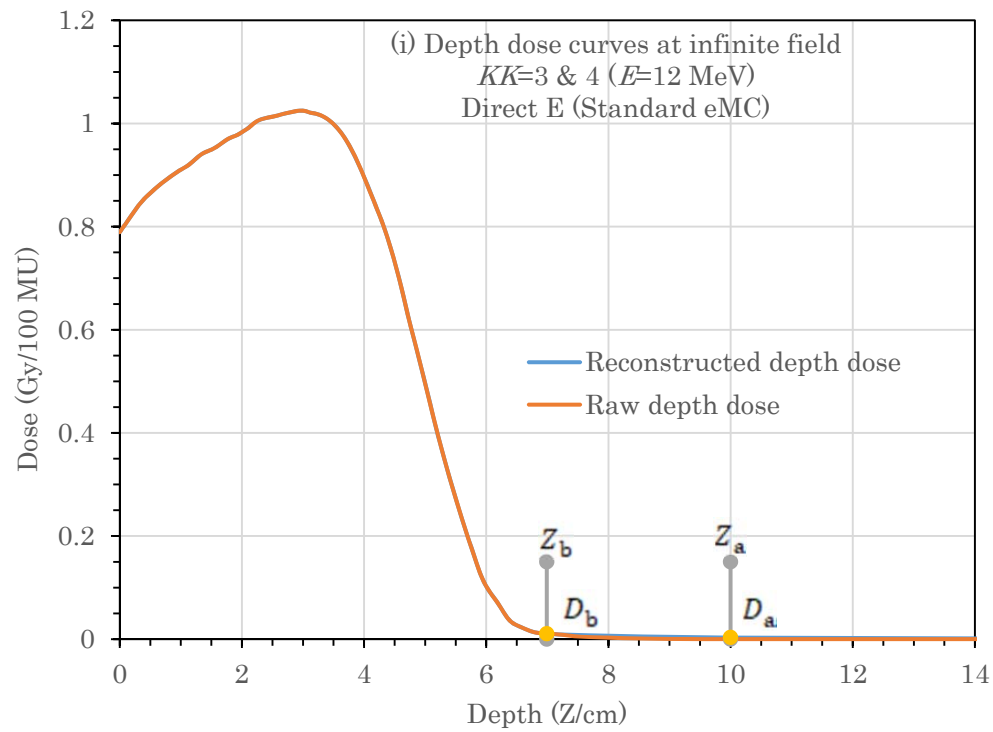
Supp. Fig. 1 Diagram showing how to reconstruct a reasonable set of doses (D_∞) at deep depths in an infinite field (in blue line) at depths of $Z \geq Z_b$, as expressed using equation 1 with datasets of $(D_a$ and $Z_a)$ and $(D_b$ and Z_b). The orange line illustrates the corresponding set of raw depth-doses.



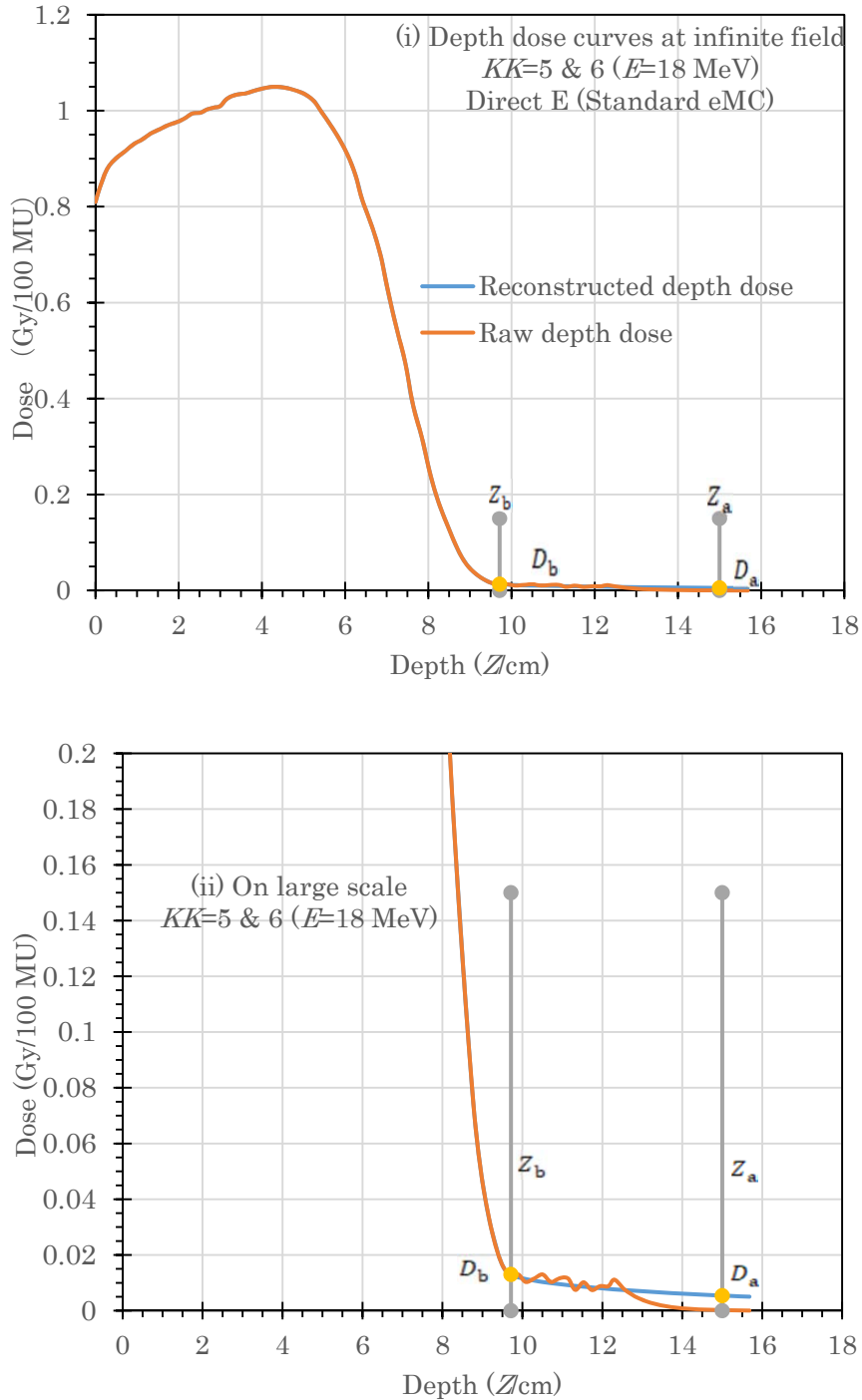
Supp. Fig. 2 Diagram showing how the effective square field ($A_c^{\text{eff}} = S_c^{\text{eff}} \times S_c^{\text{eff}}$) at each dose calculation depth (Z_c), as shaped using a square electron applicator (A_{appl}), is divided equally into small sections of 40×40 . The specific four sections surround the center (O') of the field as illustrated.



Supp. Fig. 3a

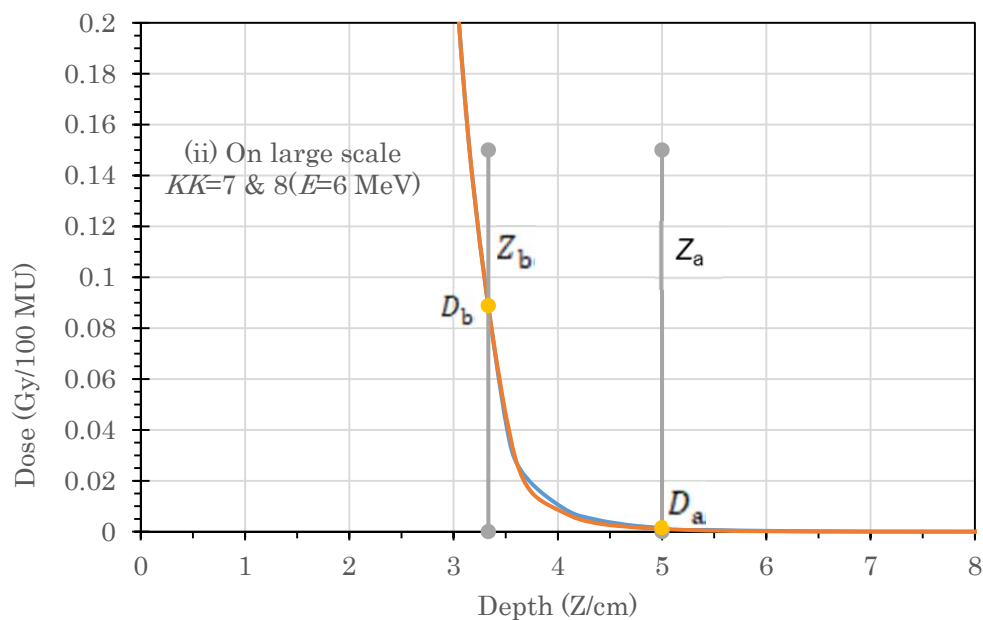
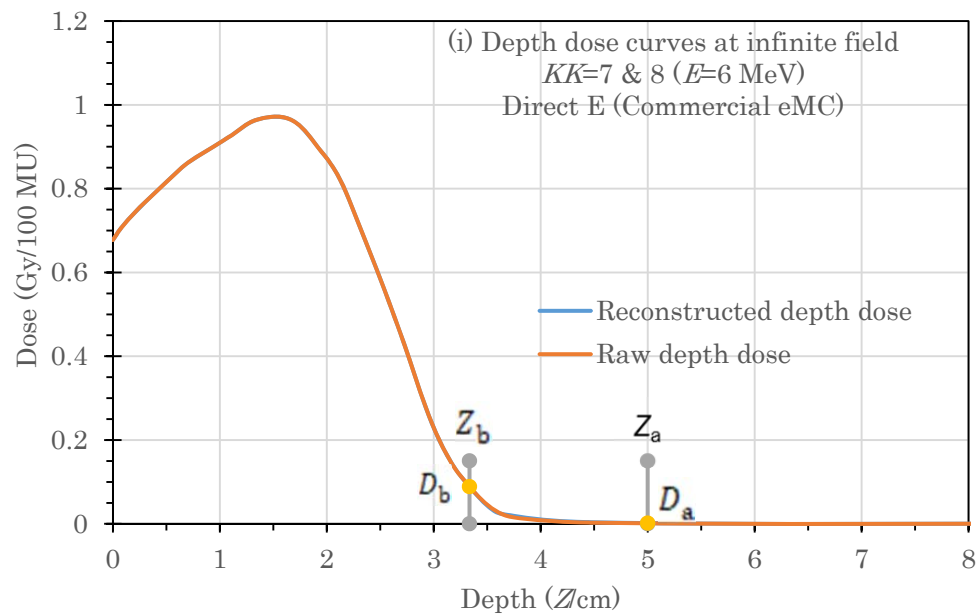


Supp. Fig. 3b

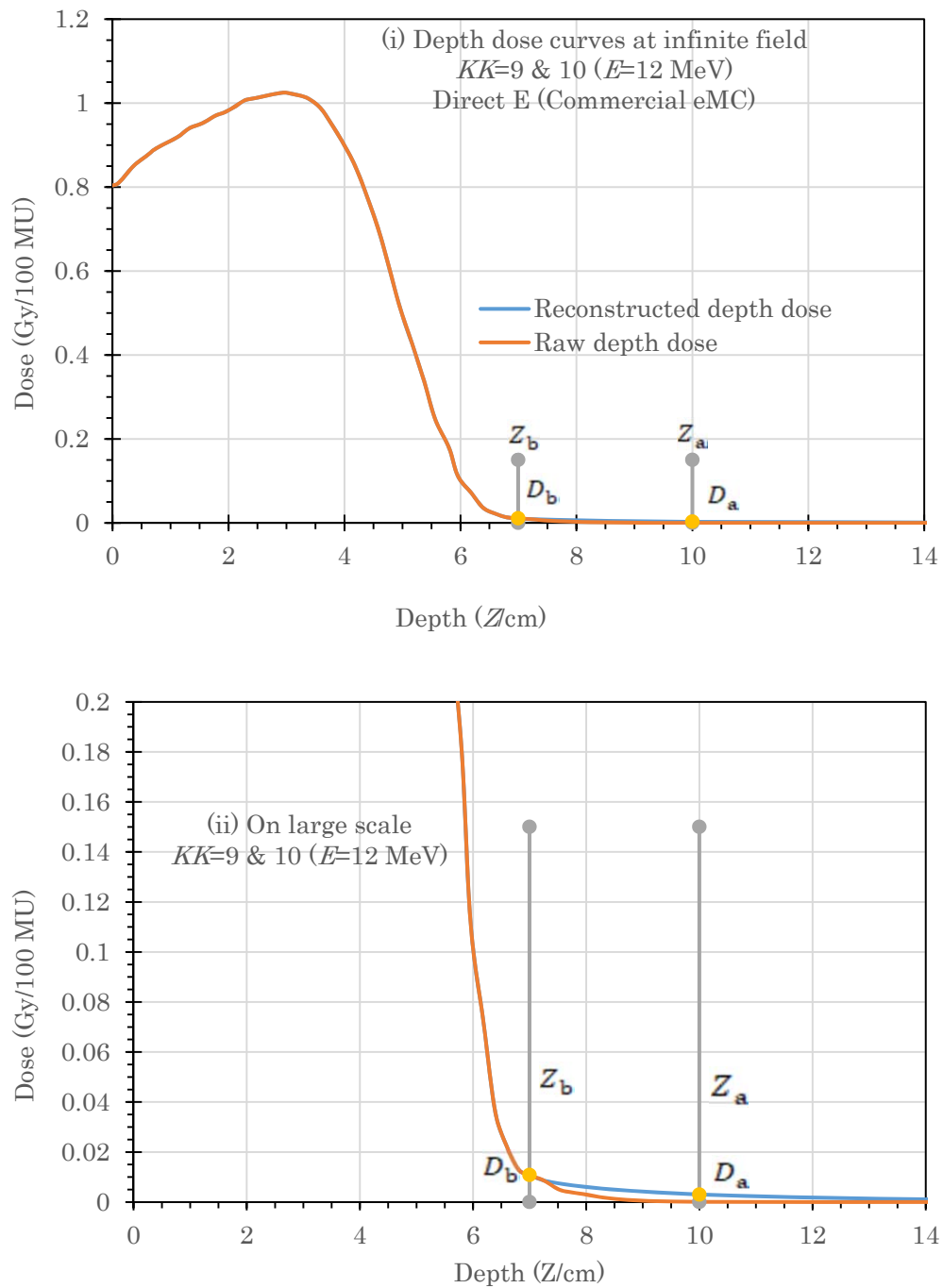


Supp. Fig. 3c

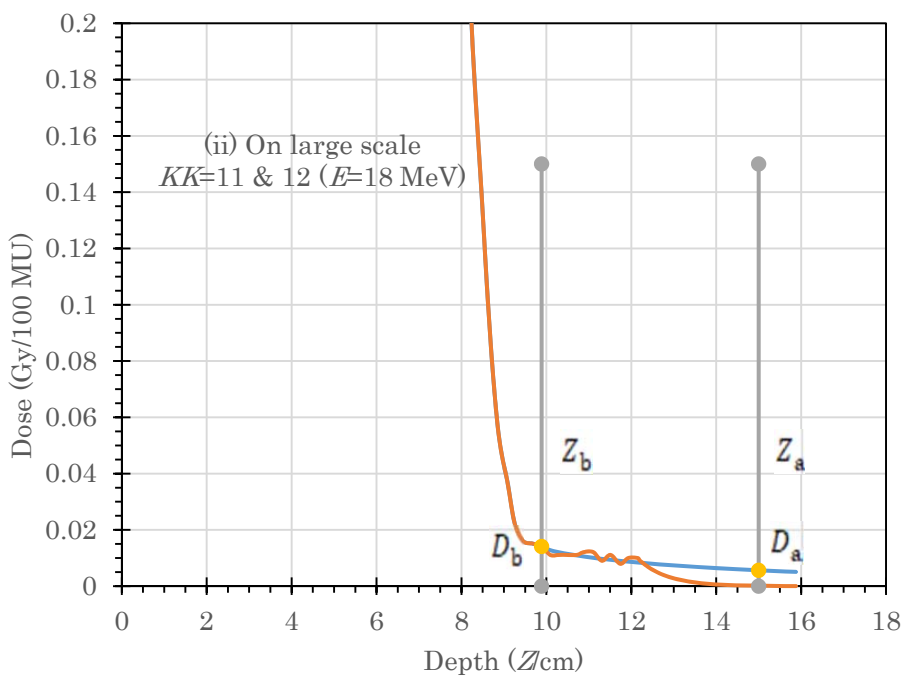
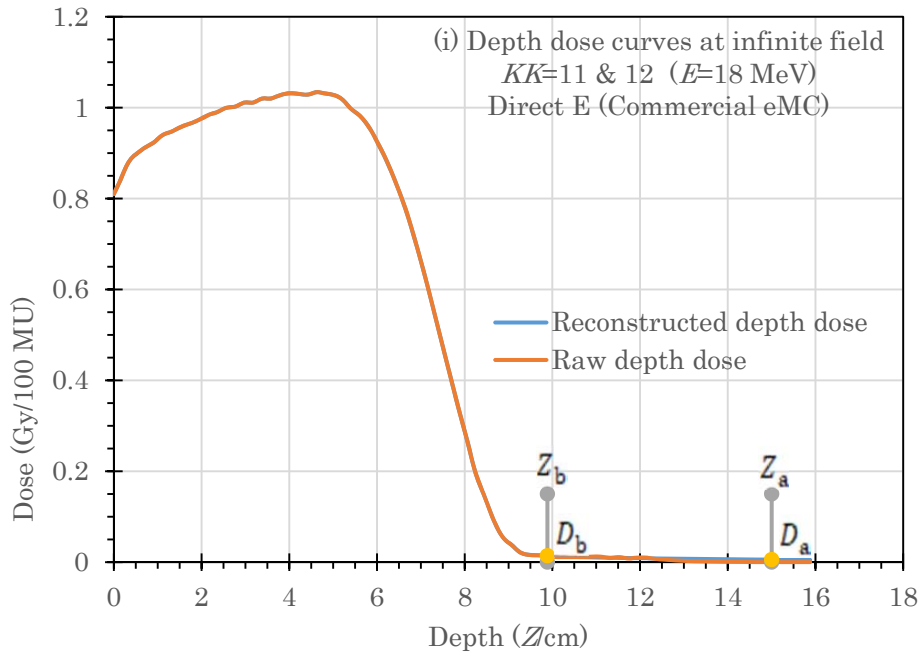
Supp. Fig. 3a-c Each set of diagrams showing how to reconstruct reasonable sets of doses (D_∞) at deep depths in an infinite field (in blue line) at depths of $Z \geq Z_b$ using datasets of $(D_a \text{ and } Z_a)$ and $(D_b \text{ and } Z_b)$ for (a) $KK=1 \text{ & } 2$ (6 MeV), (b) $KK=3 \text{ & } 4$ (12 MeV), or (c) $KK=5 \text{ & } 6$ (18 MeV), produced for *direct electron beams on the standard eMC*.



Supp. Fig. 4a

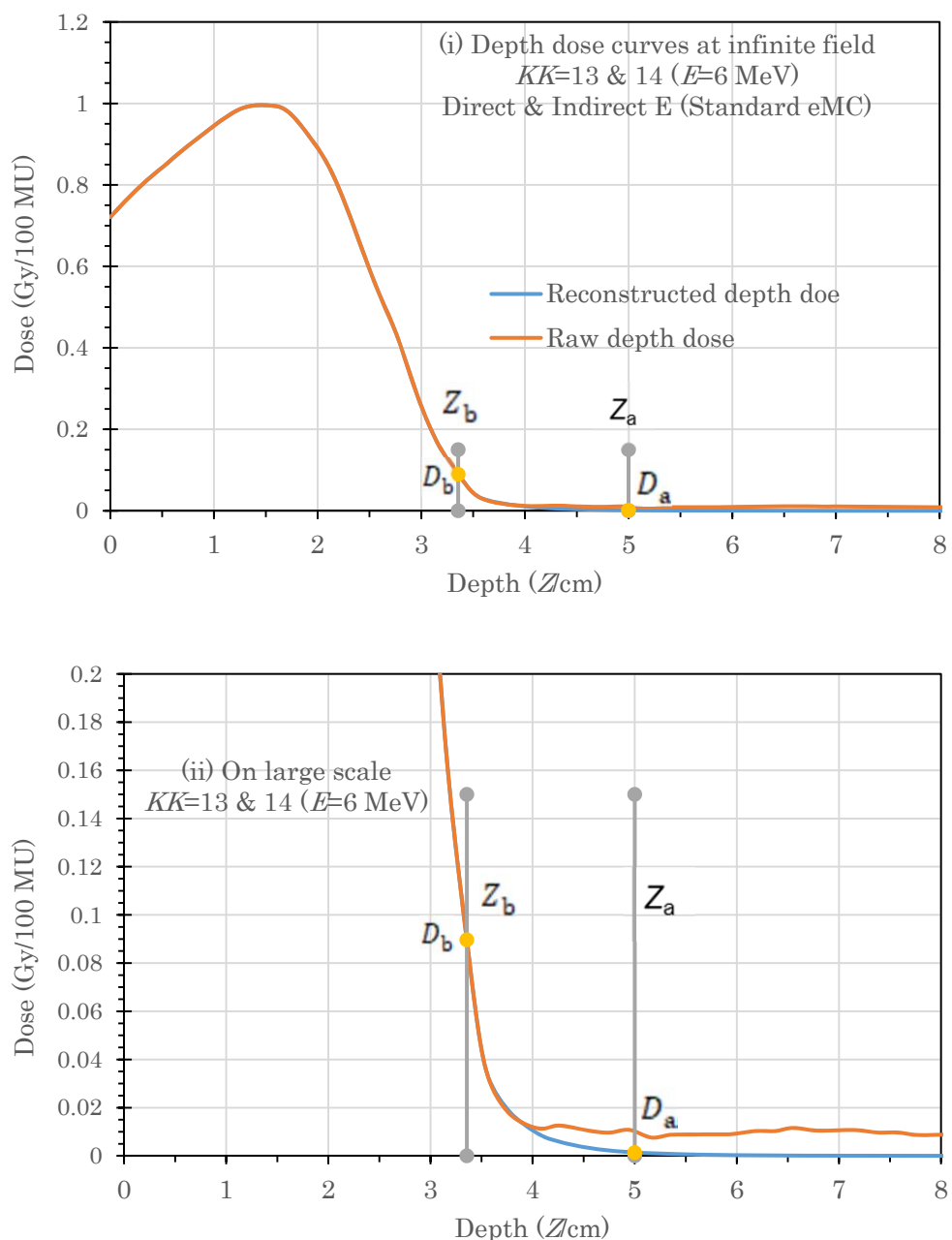


Supp. Fig. 4b

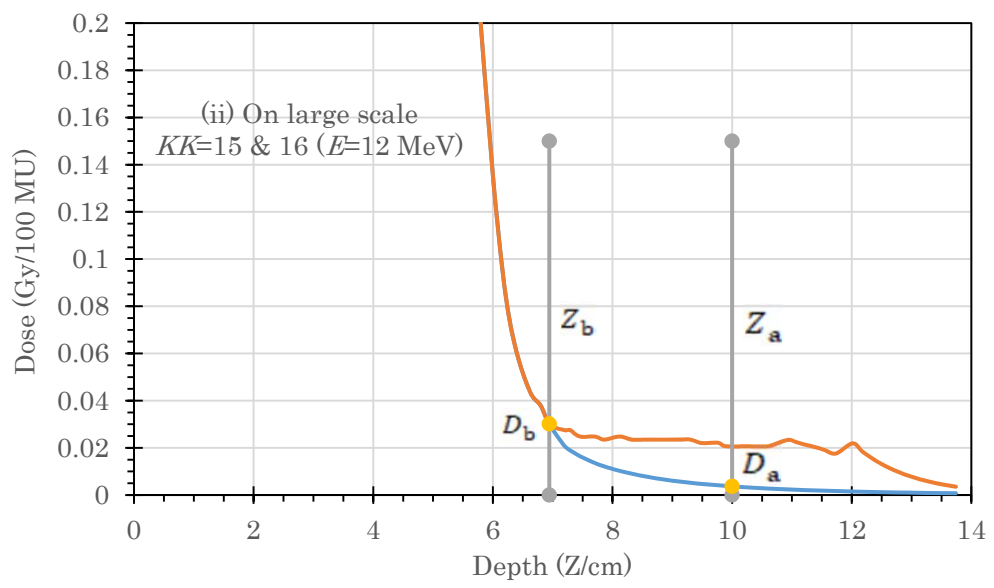
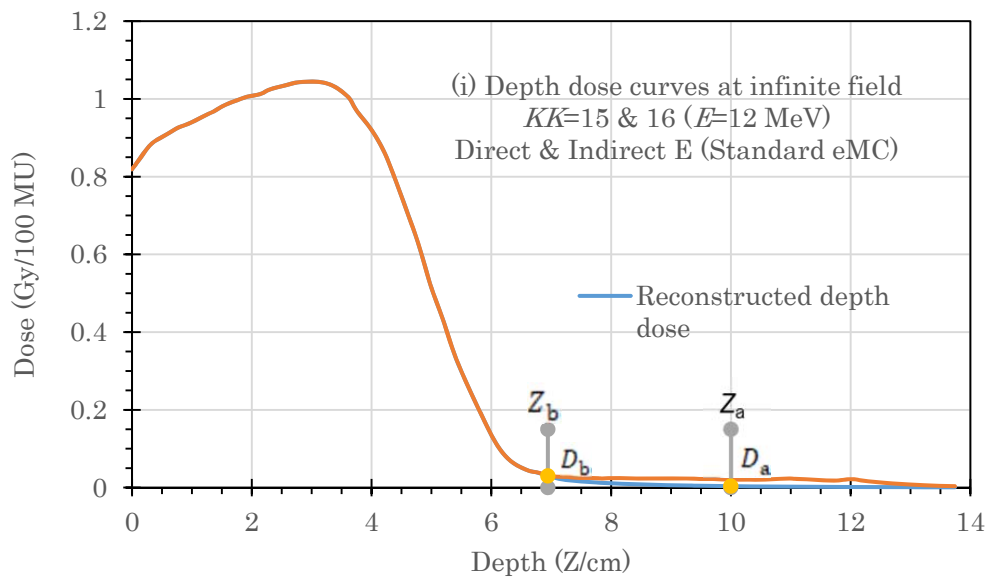


Supp. Fig. 4c

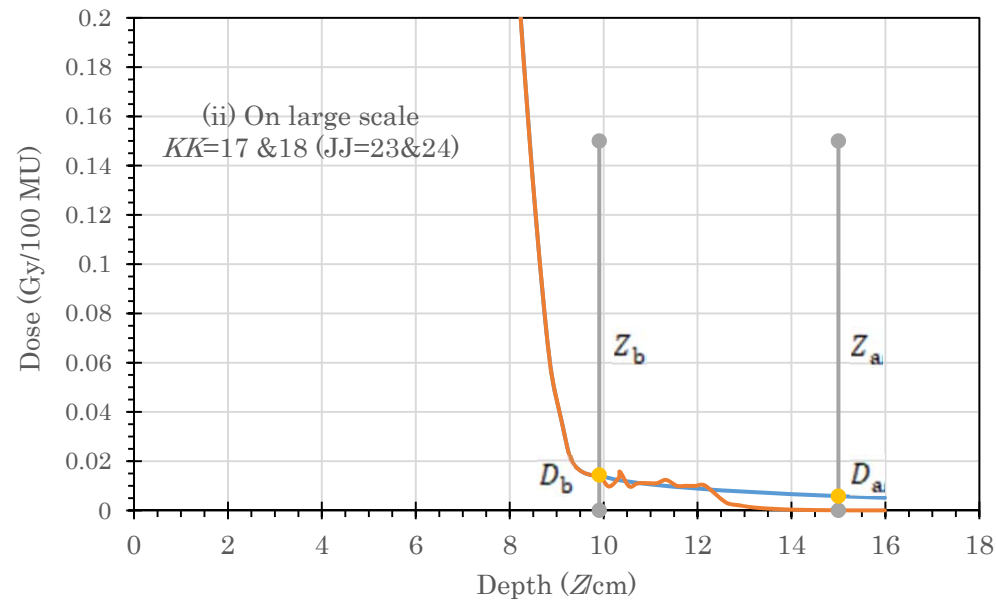
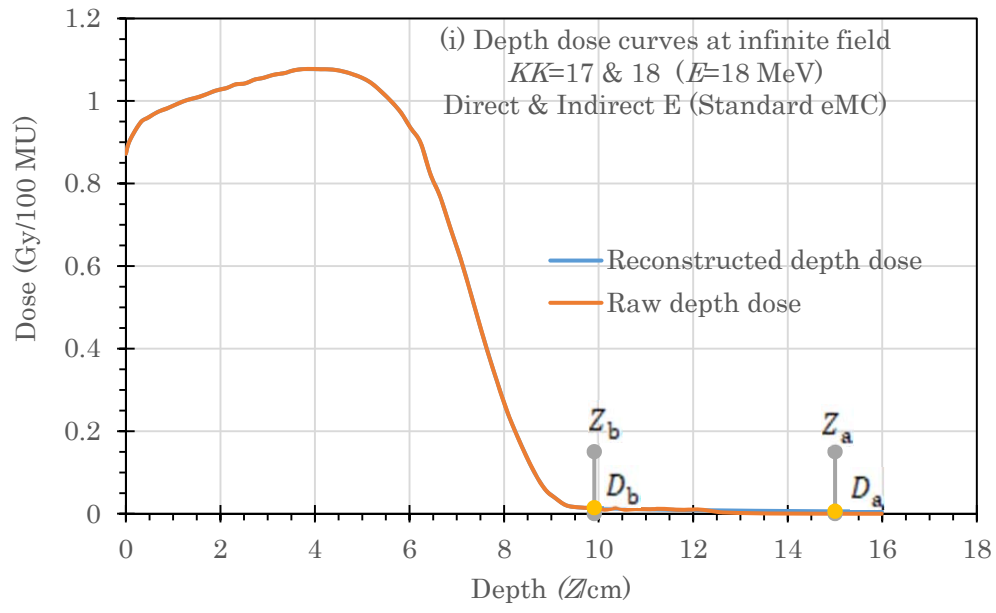
Supp. Fig. 4a-c Each set of diagrams for (a) $KK=7 \text{ & } 8$ (6 MeV), (b) $KK=9 \text{ & } 10$ (12 MeV), or (c) $KK=11 \text{ & } 12$ (18 MeV), produced for *direct electron beams* on the *commercial eMC* using the same way as in Figure 3.



Supp. Fig. 5a

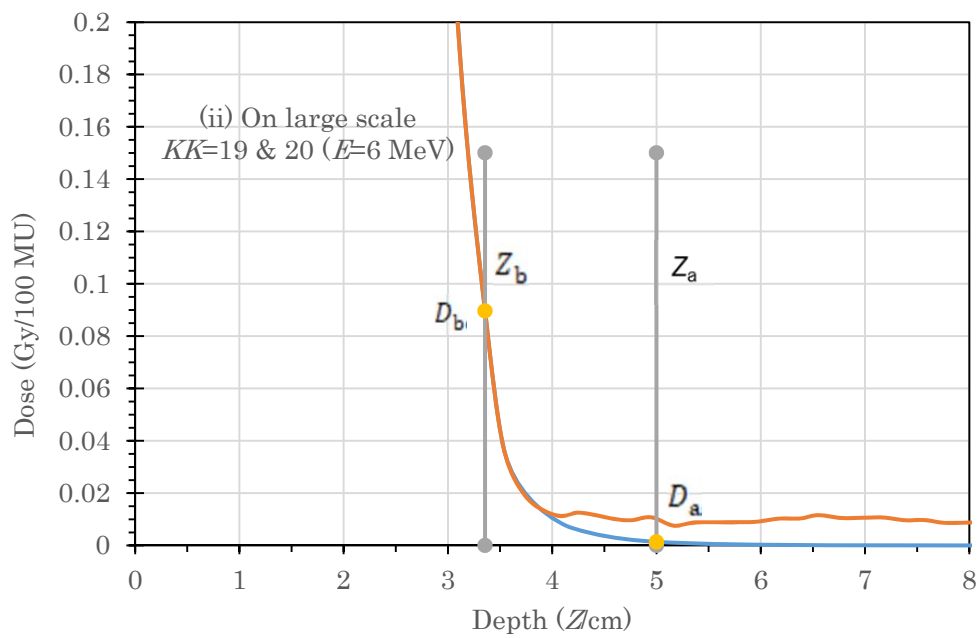
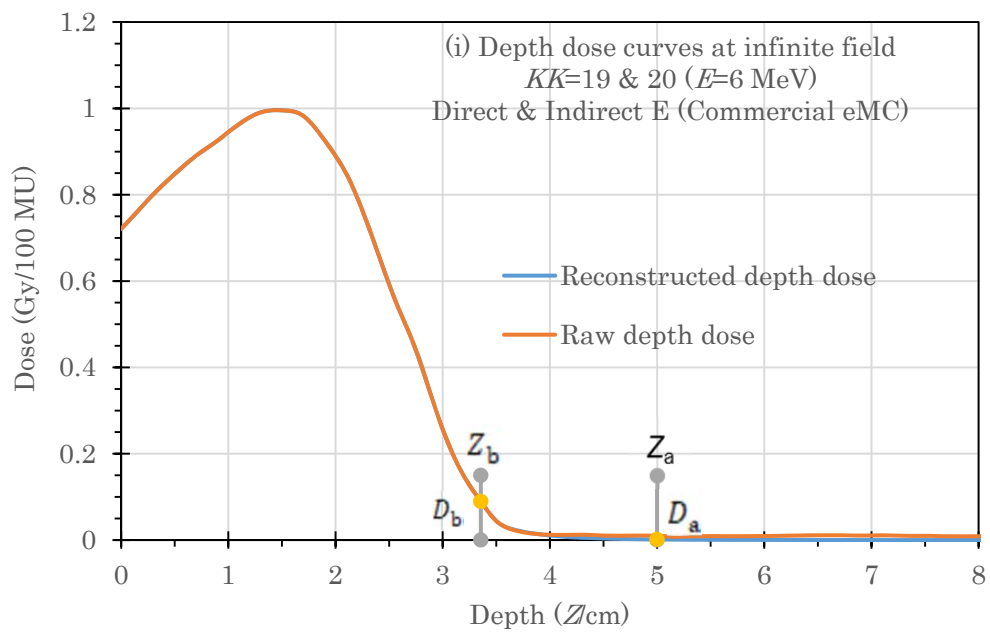


Supp. Fig. 5b

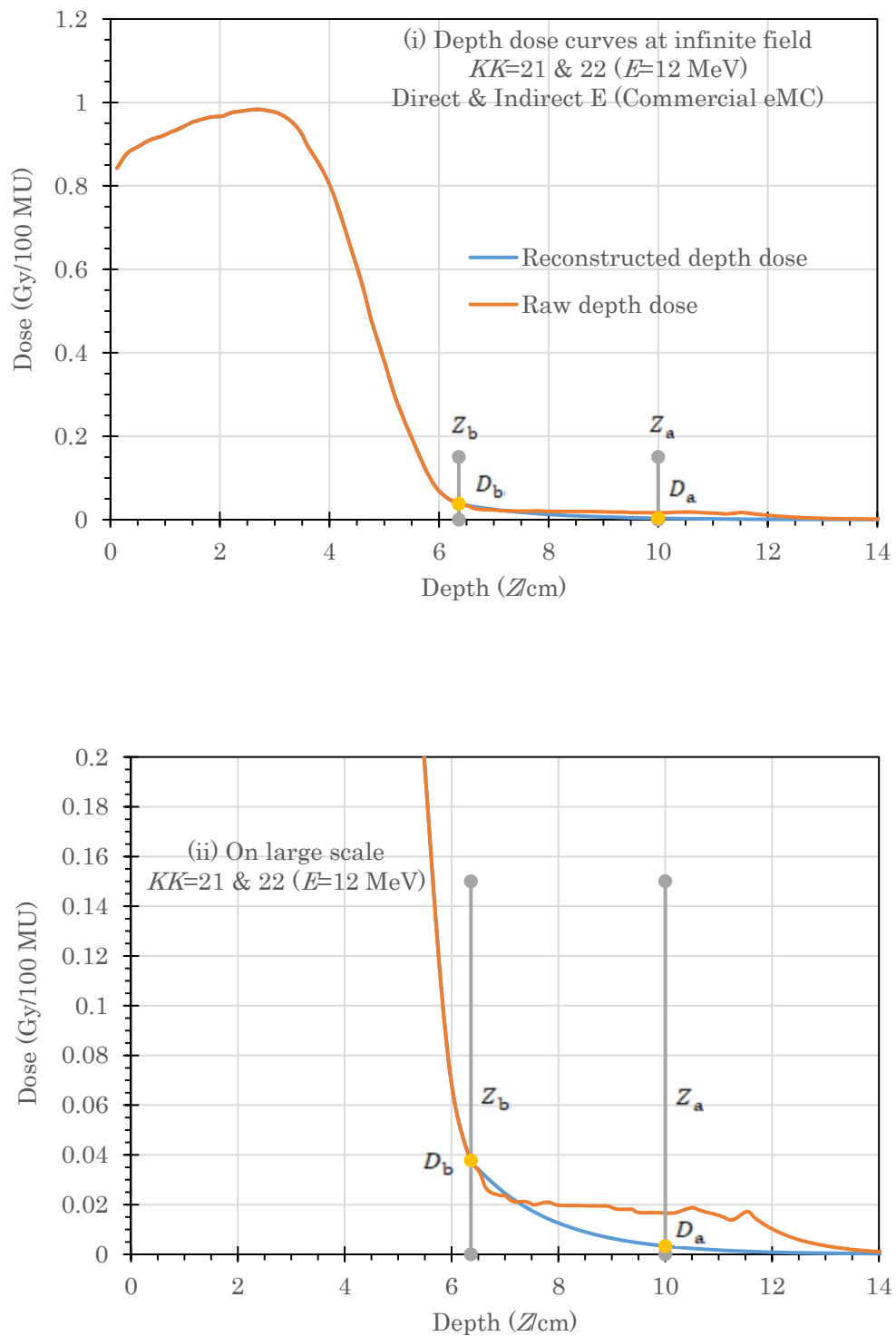


Supp. Fig. 5c

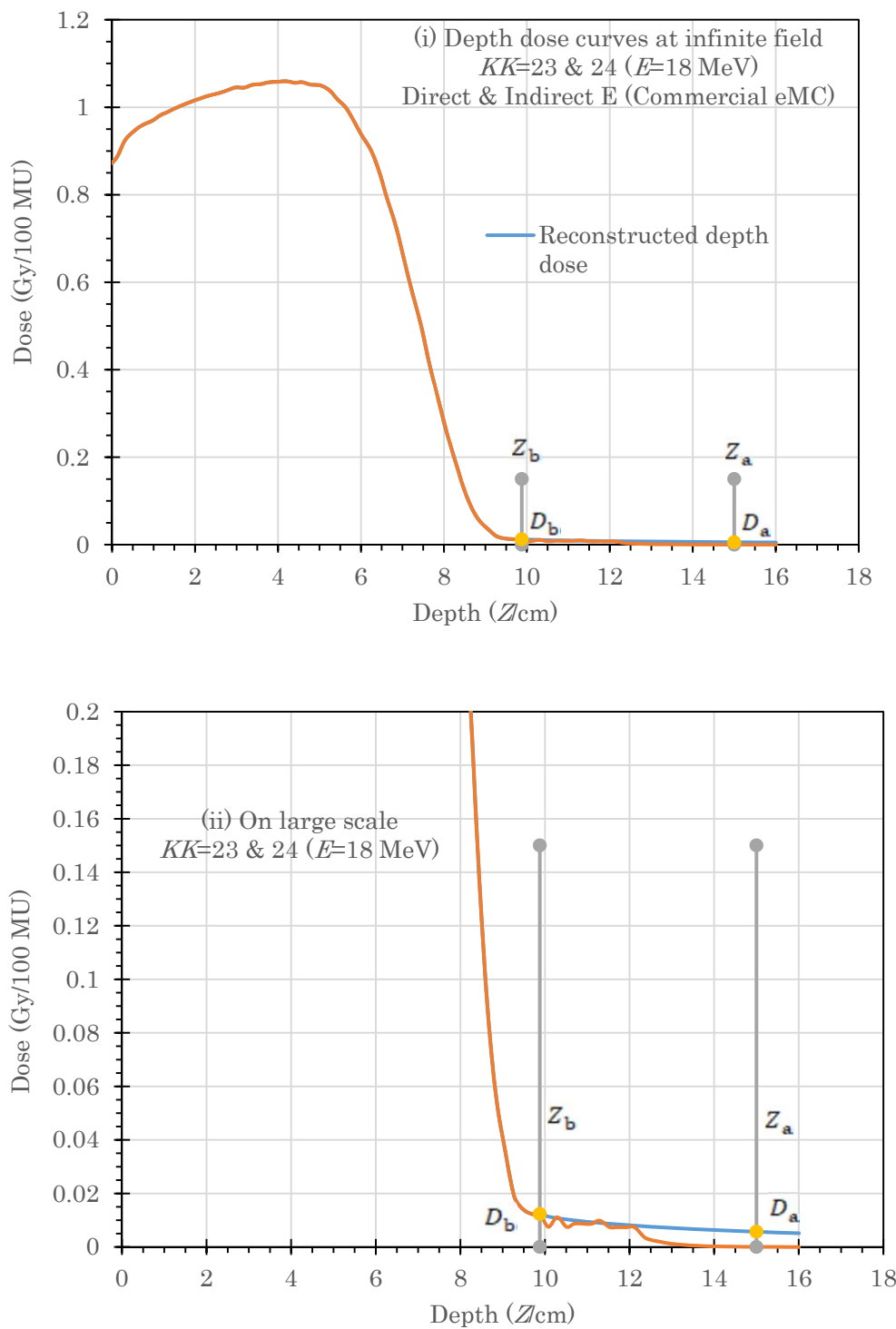
Supp. Fig. 5a-c Each set of diagrams for (a) $KK=13 \text{ & } 14$ (6 MeV), (b) $KK=15 \text{ & } 16$ (12 MeV), or (c) $KK=17 \text{ & } 18$ (18 MeV), produced for *direct & indirect electron beams* on the *standard eMC* using the same way as in Figure 3.



Supp. Fig. 6a

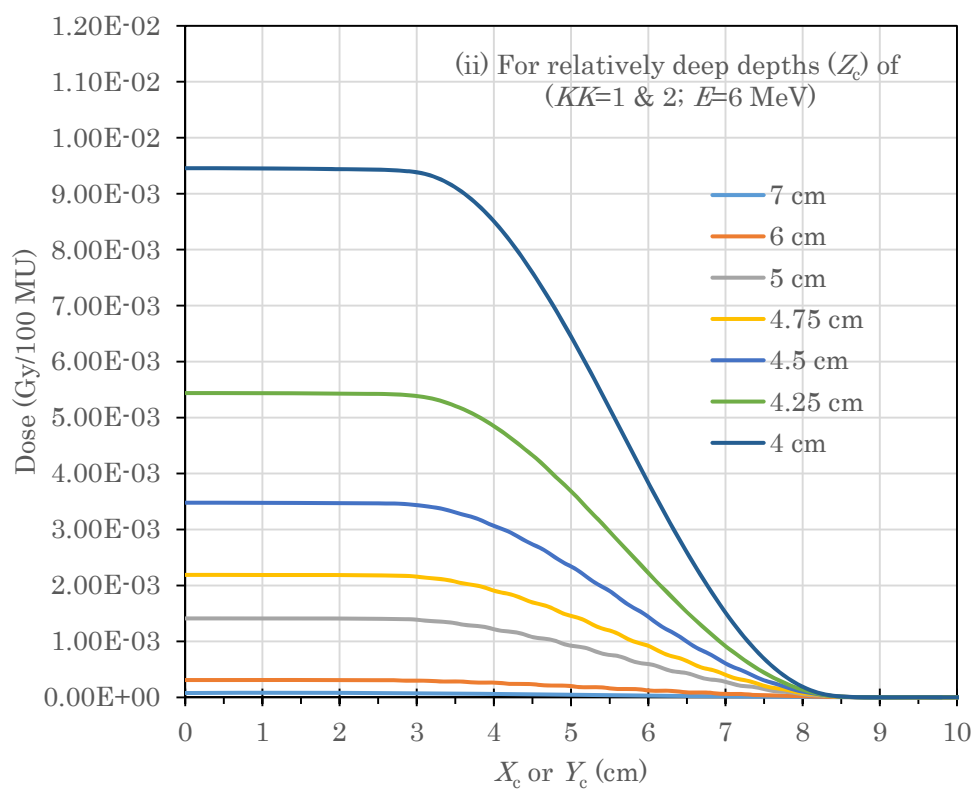
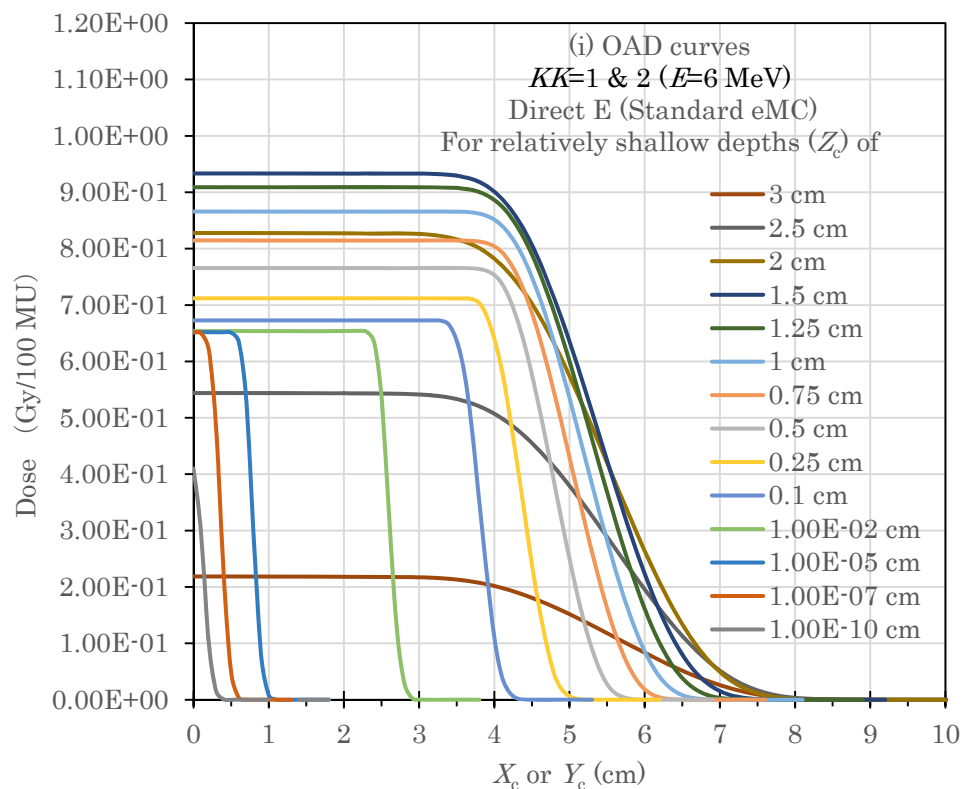


Supp. Fig. 6b

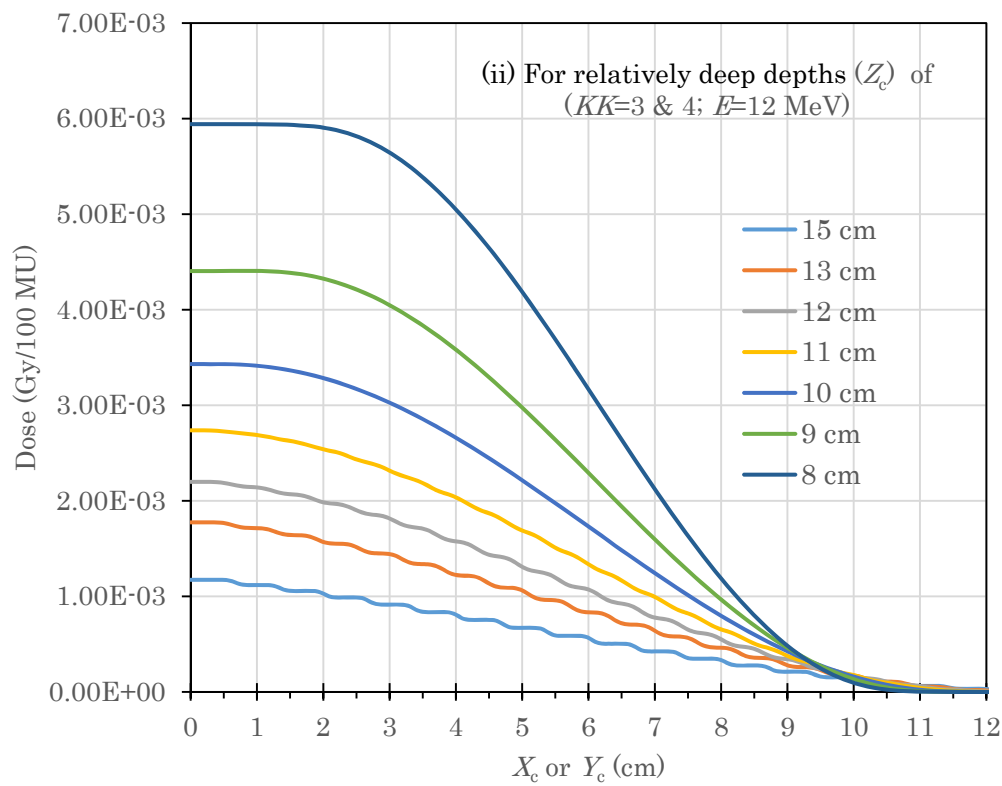
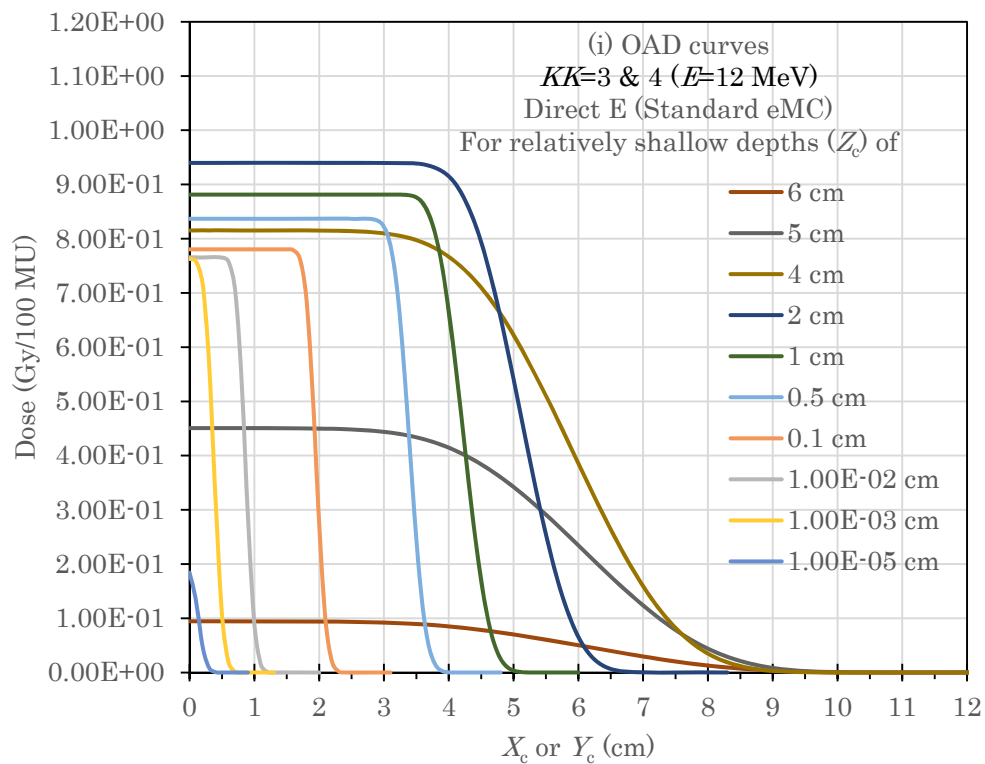


Supp. Fig. 6c

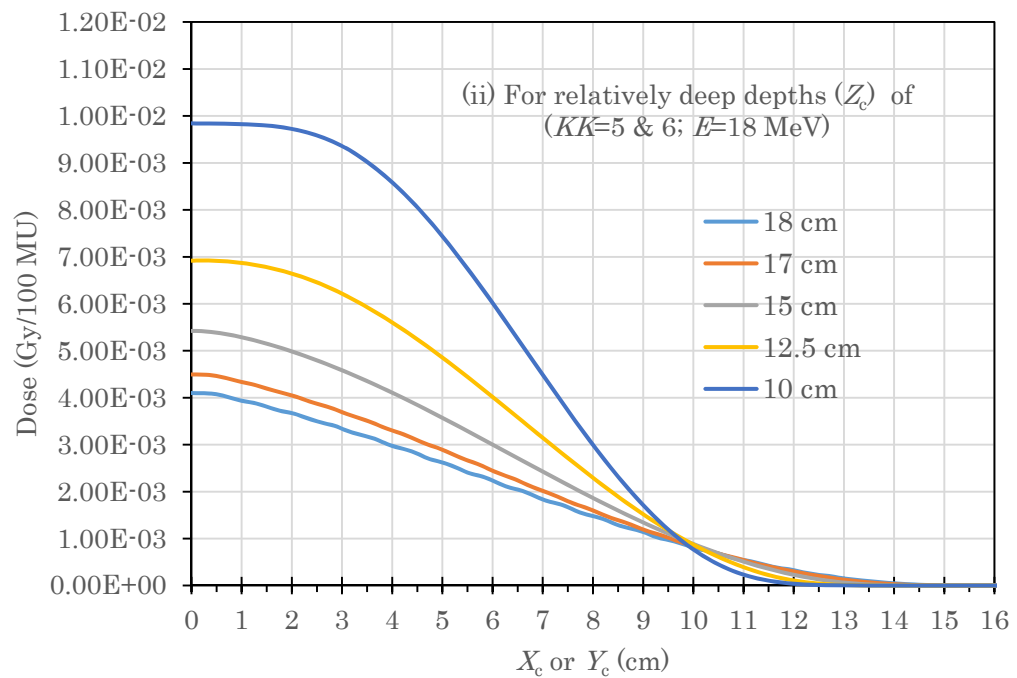
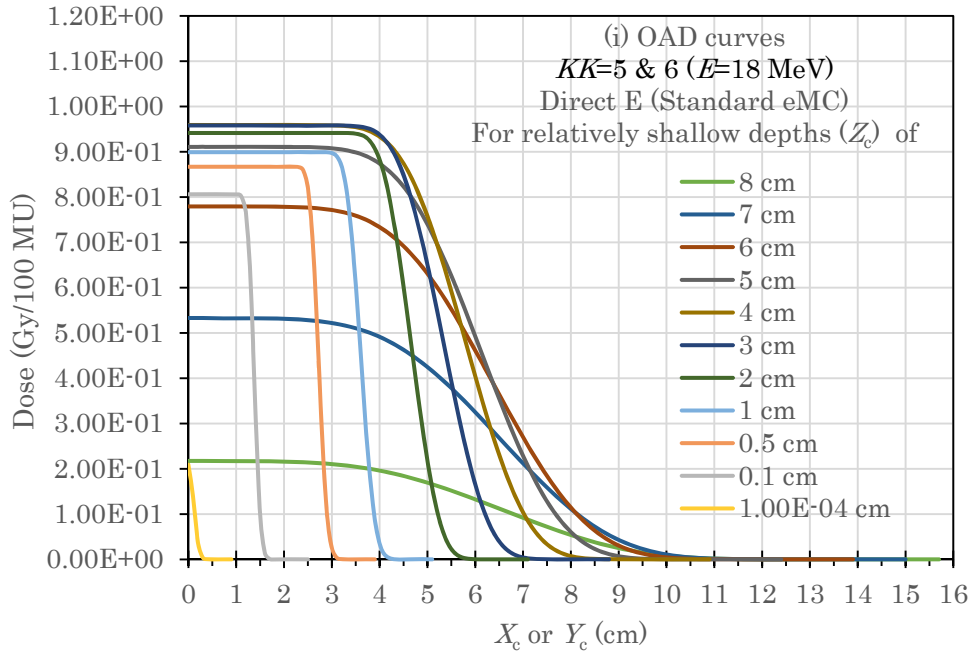
Supp. Fig. 6a-c Each set of diagrams for (a) $KK=19 \text{ & } 20$ (6 MeV), (b) $KK=21 \text{ & } 22$ (12 MeV), or (c) $KK=23 \text{ & } 24$ (18 MeV), produced for *direct & indirect electron* beams on the *commercial eMC* using the same way as in Figure 3.



Supp. Fig. 7a

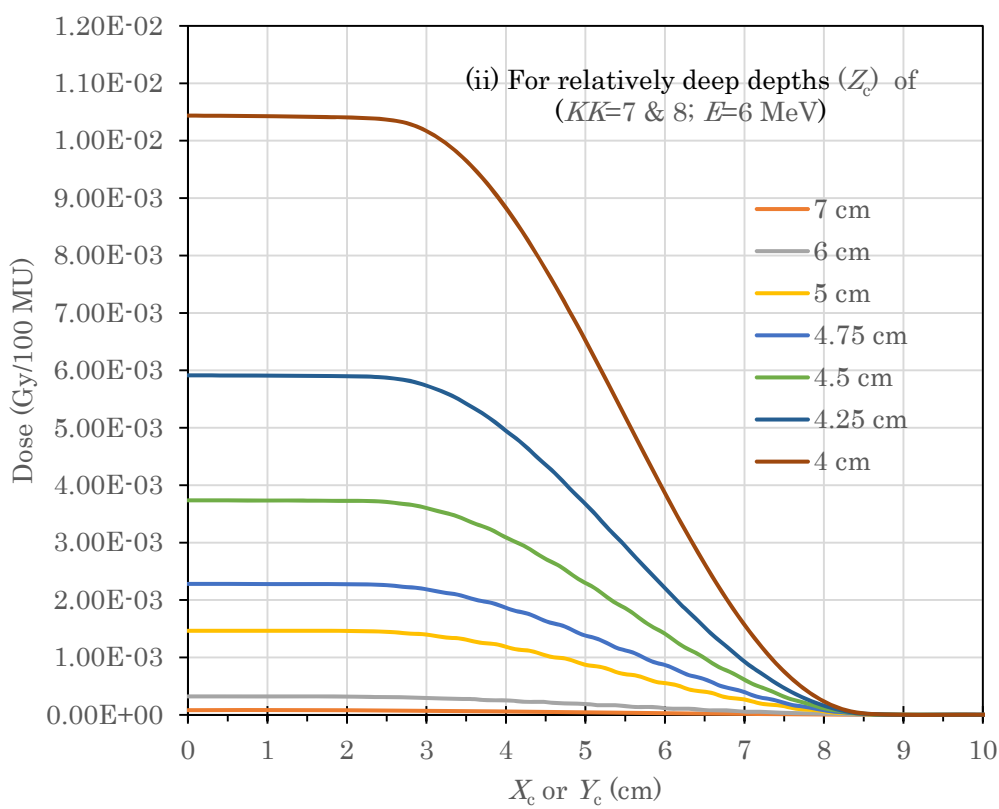
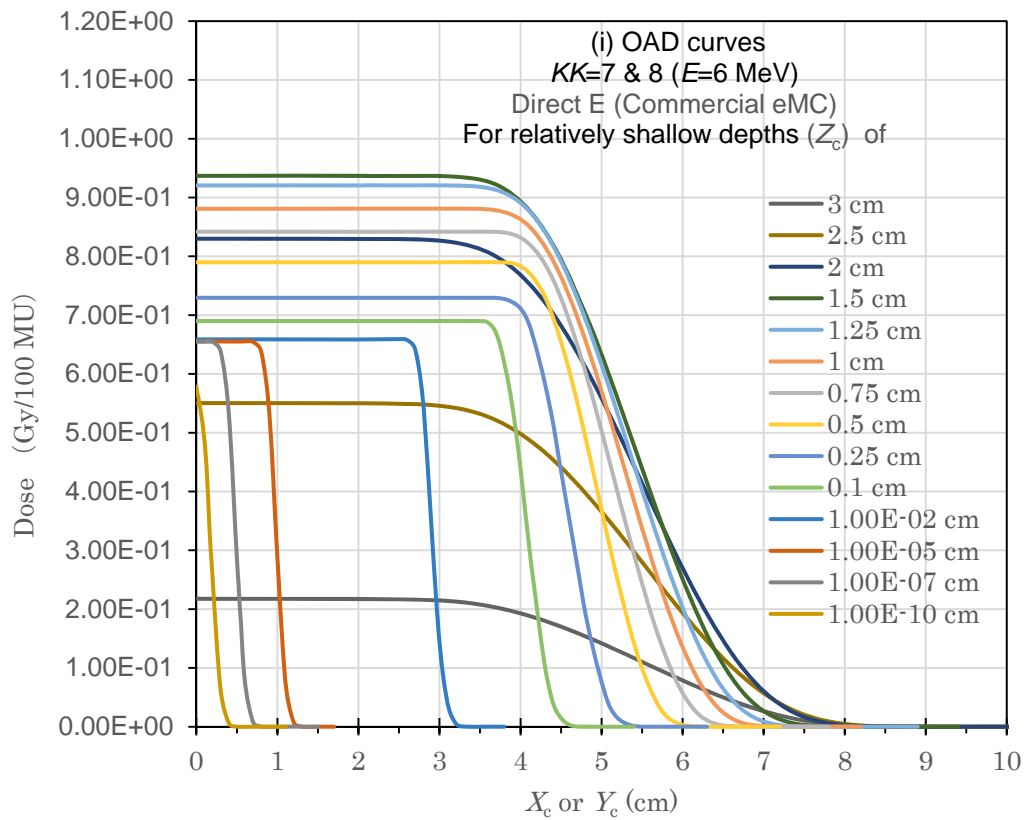


Supp. Fig. 7b

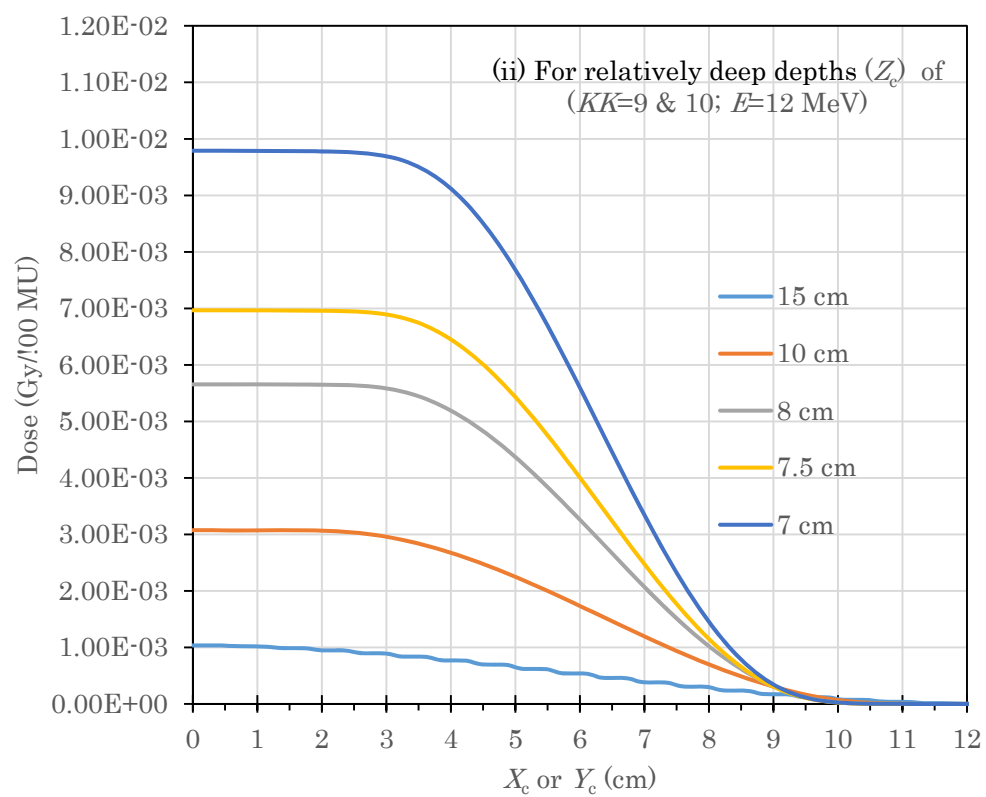
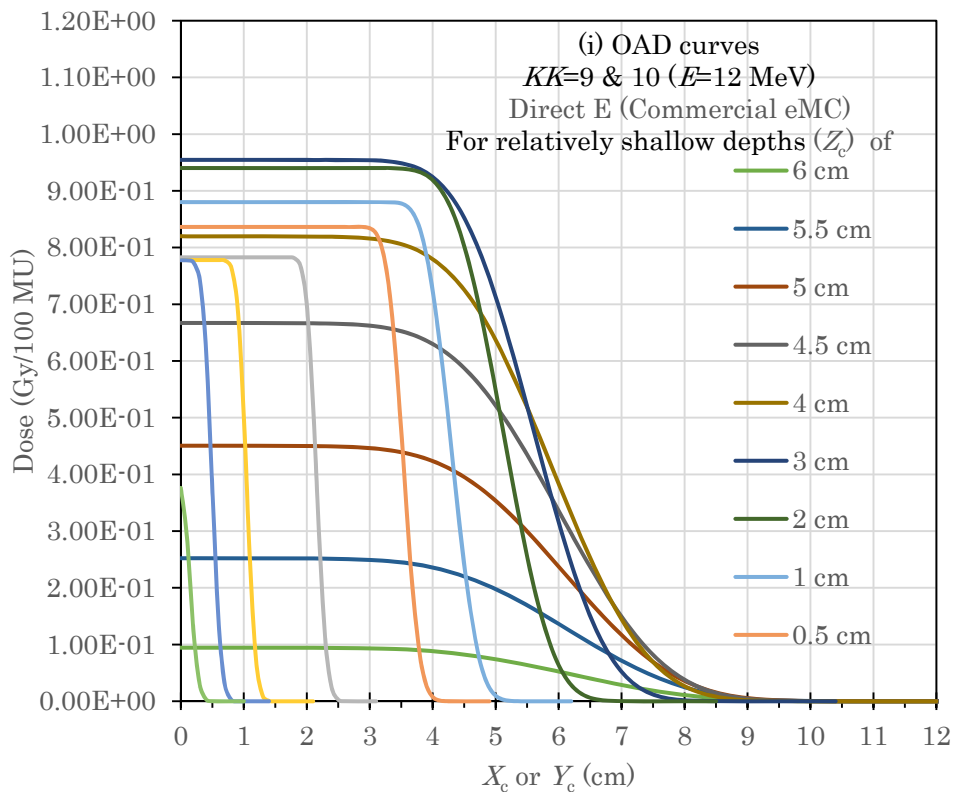


Supp. Fig. 7c

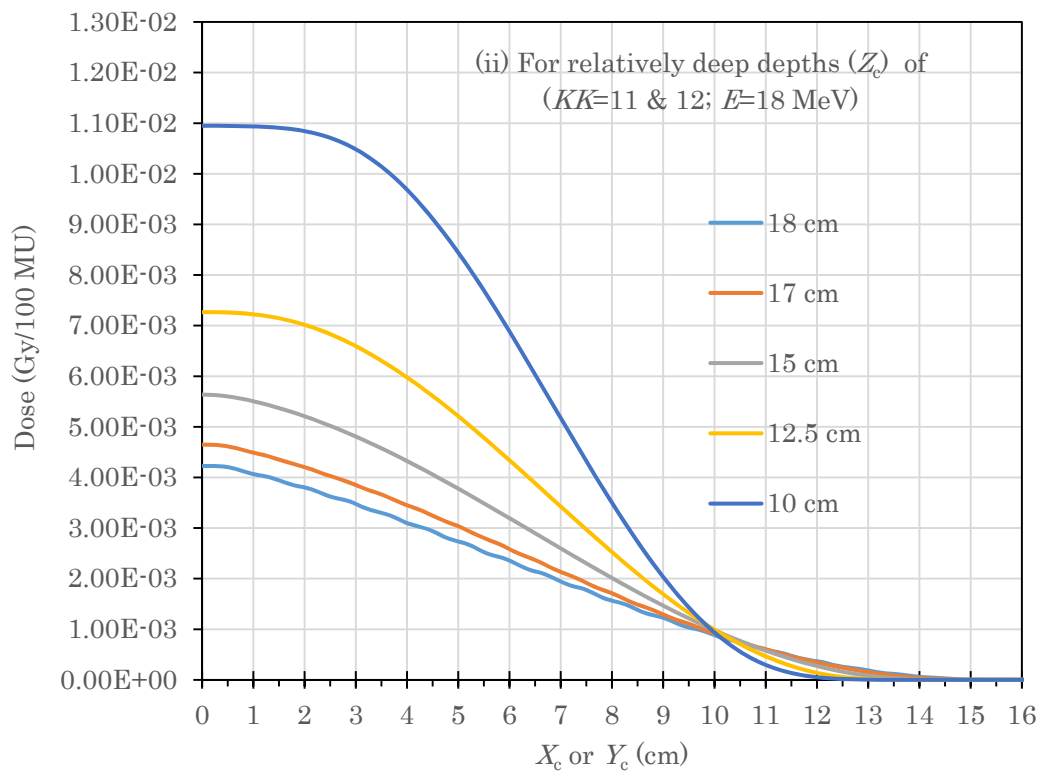
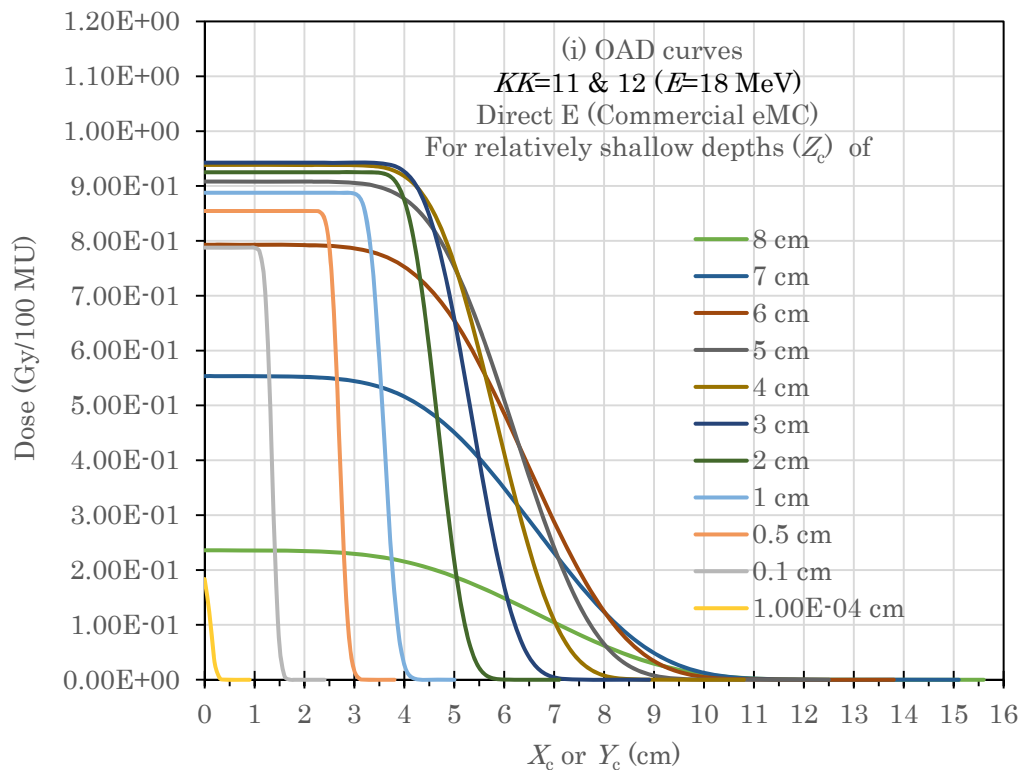
Supp. Fig. 7a-c Each set of diagrams showing how the OAD dataset varies with the X_c or Y_c distance on each horizontal surface for (a) $KK=1 \text{ & } 2$ (6 MeV), (b) $KK=3 \text{ & } 4$ (12 MeV), or (c) $KK=5 \text{ & } 6$ (18 MeV), produced for direct Electron beams on the standard eMC. The datasets are divided into two groups of (i) and (ii) according to the Z_c depth.



Supp. Fig. 8a

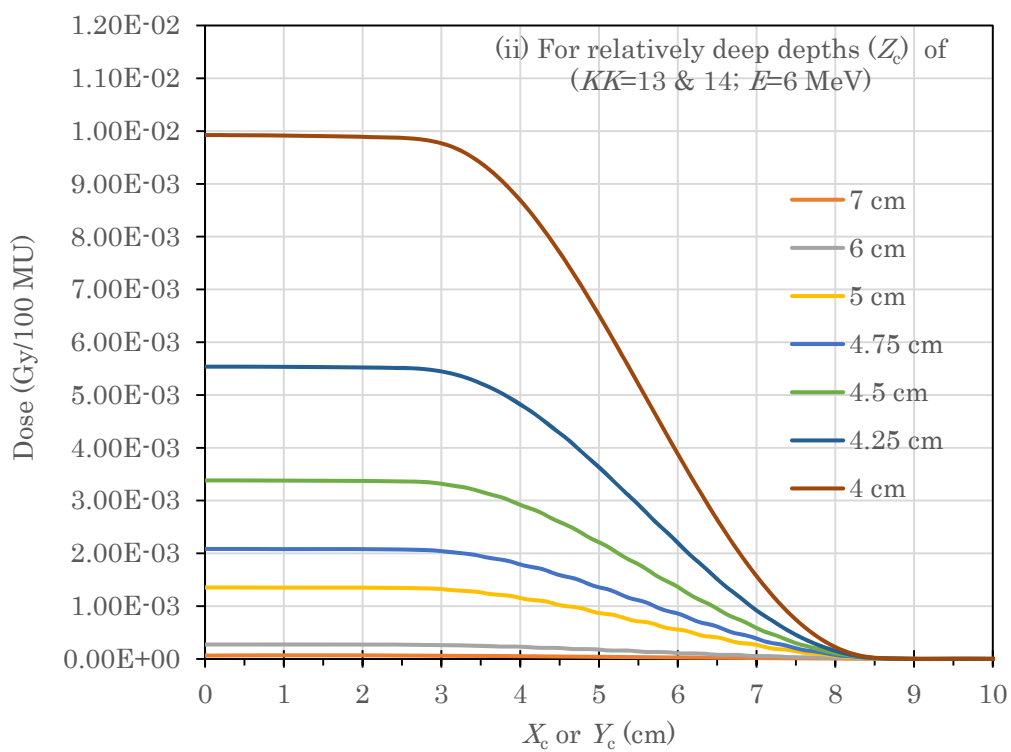
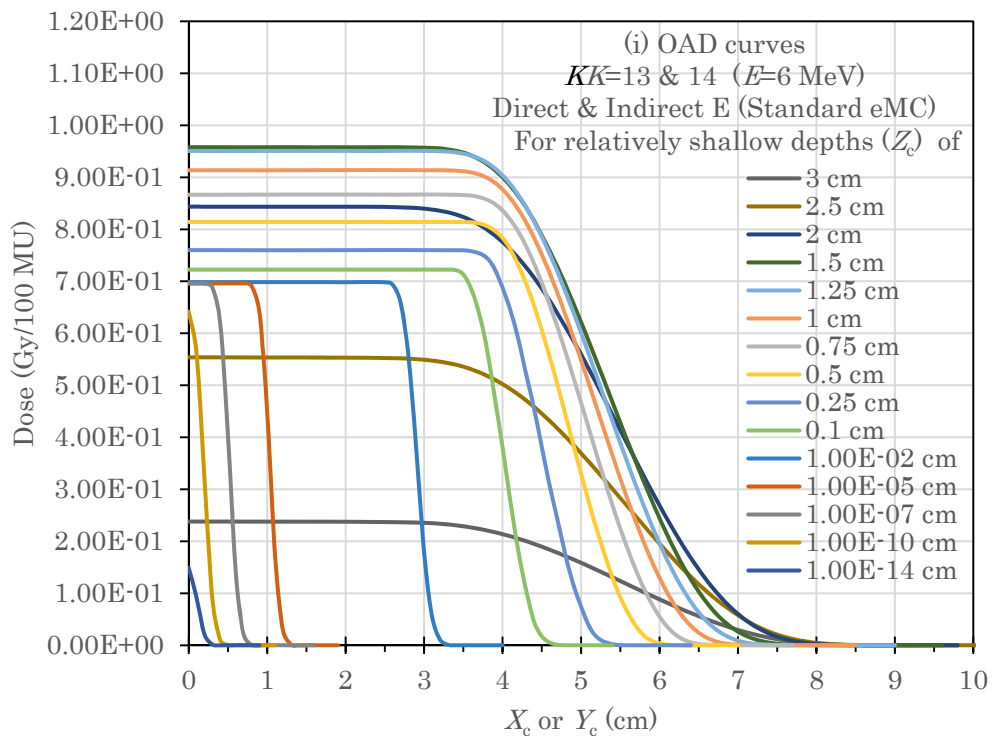


Supp. Fig. 8b

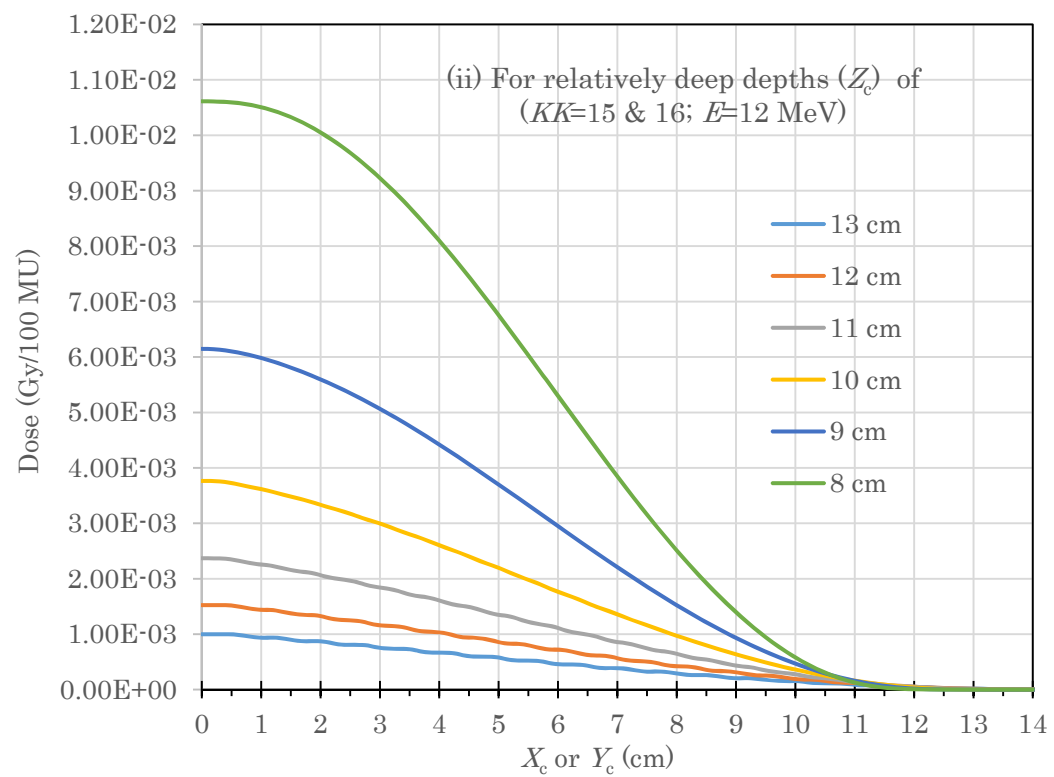
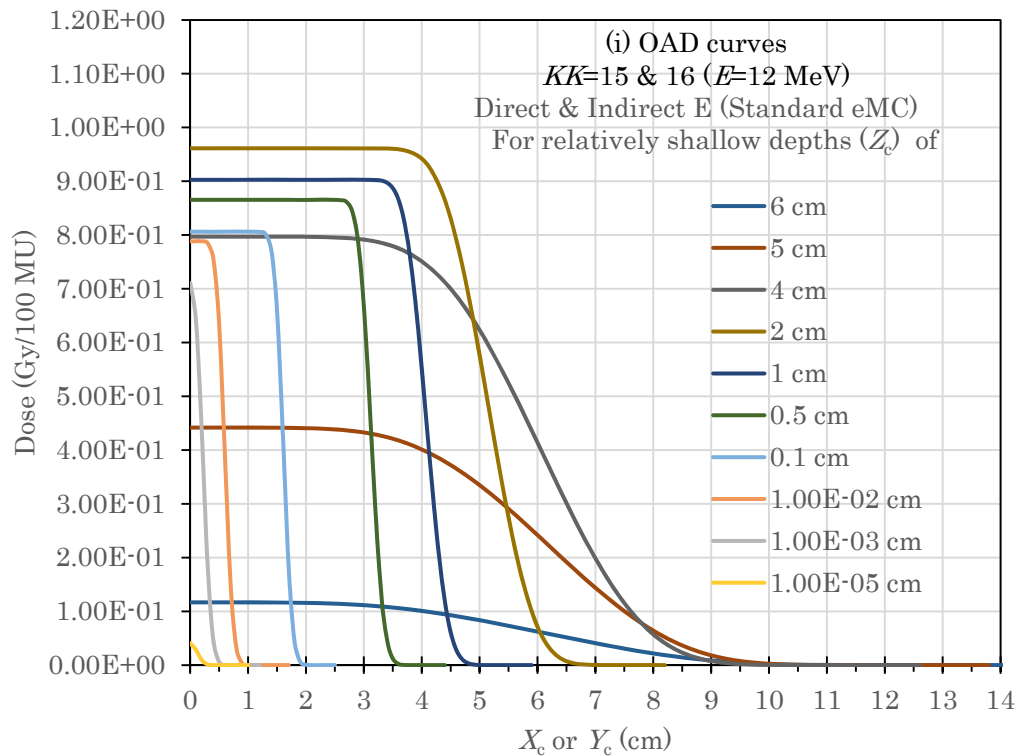


Supp. Fig. 8c

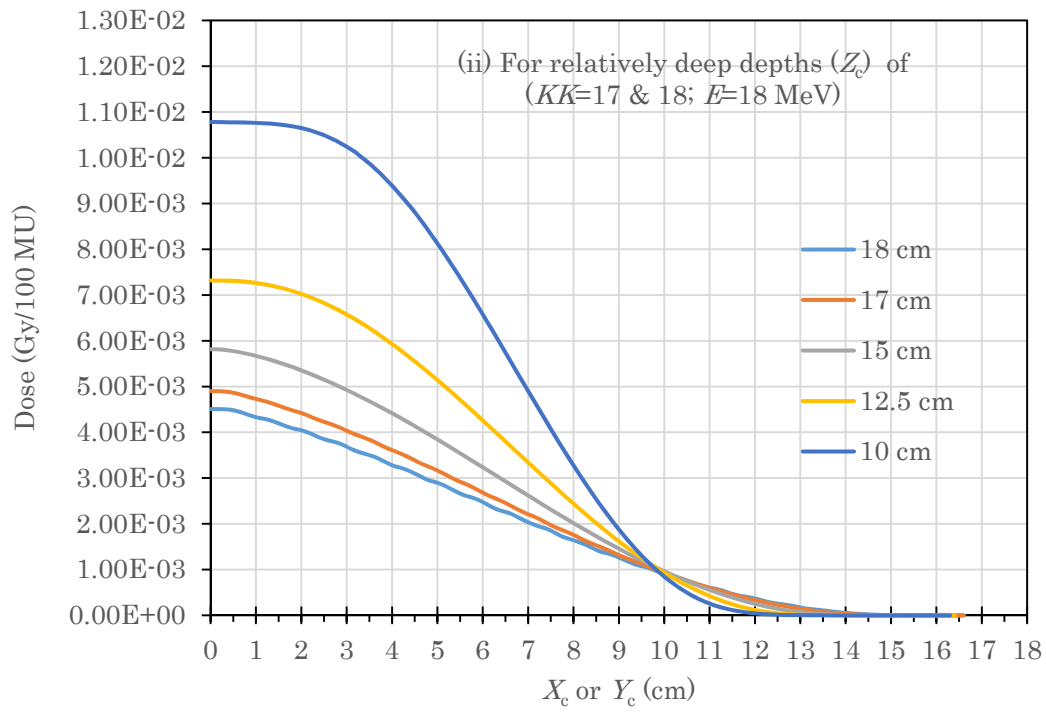
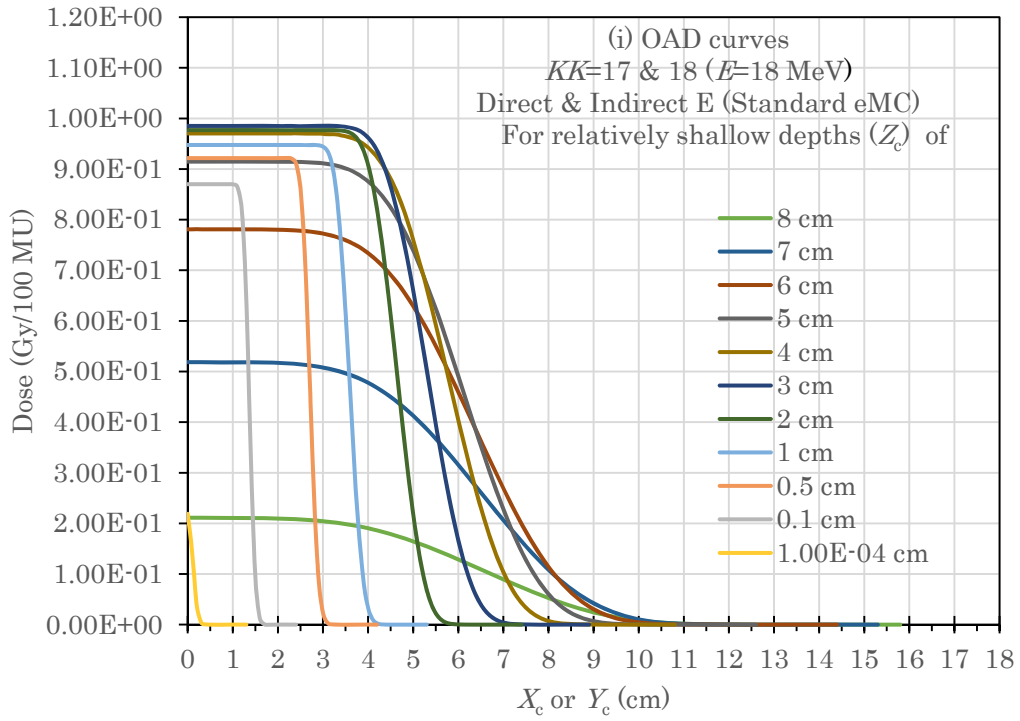
Supp. Fig. 8a-c Each set of diagrams for (a) $KK=7 \text{ & } 8$ (6 MeV), (b) $KK=9 \text{ & } 10$ (12 MeV), or (c) $KK=11 \text{ & } 12$ (18 MeV), produced for *direct electron beams* on the *commercial eMC* using the same way as in Figure 7.



Supp. Fig. 9a

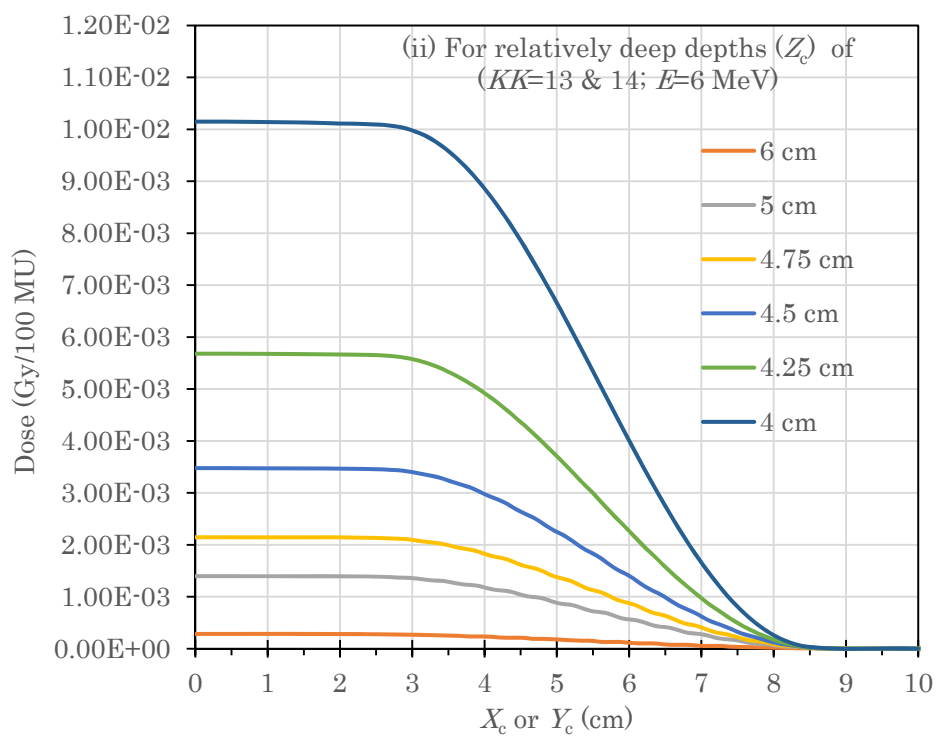
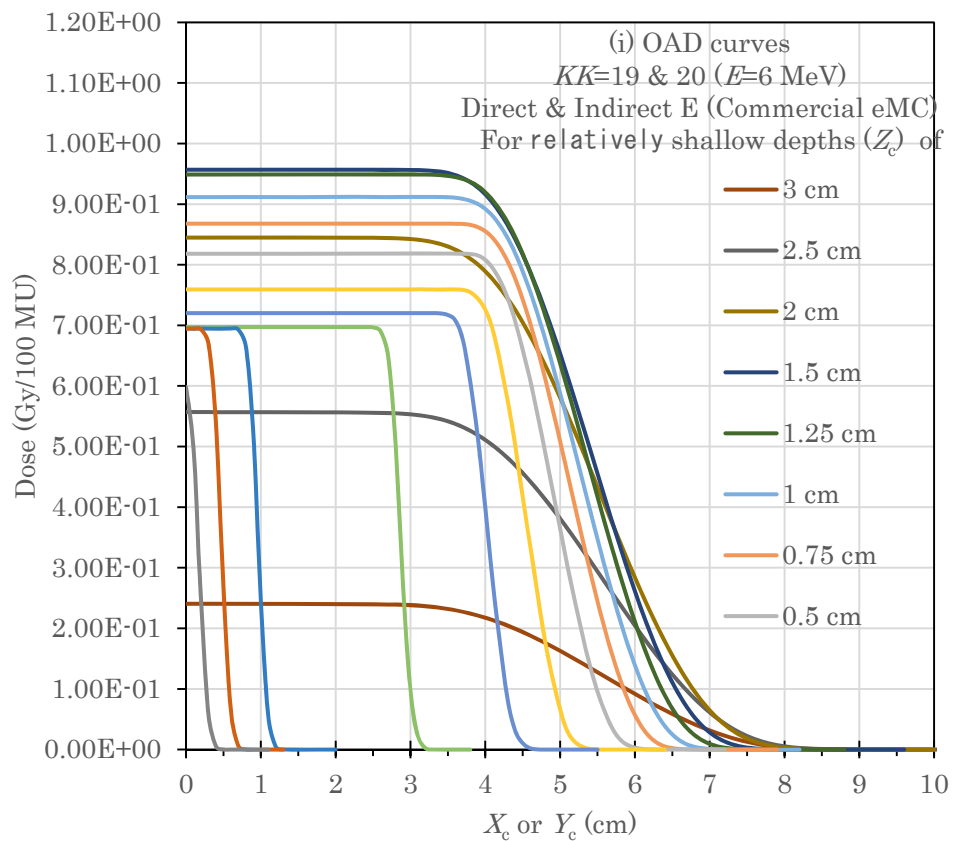


Supp. Fig. 9b

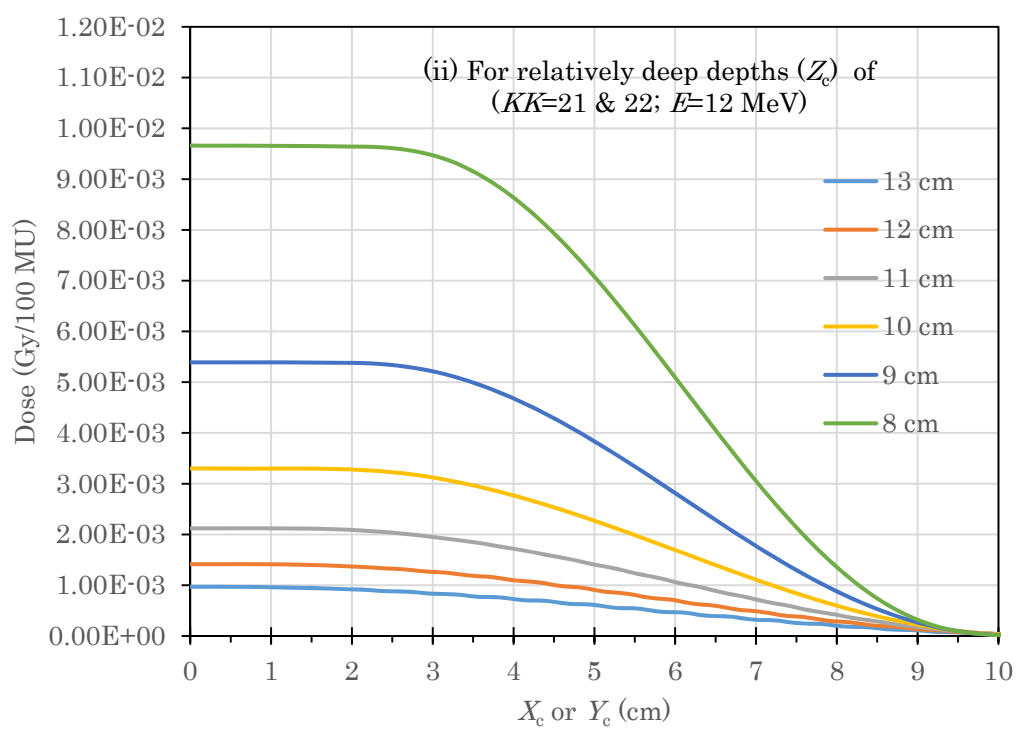
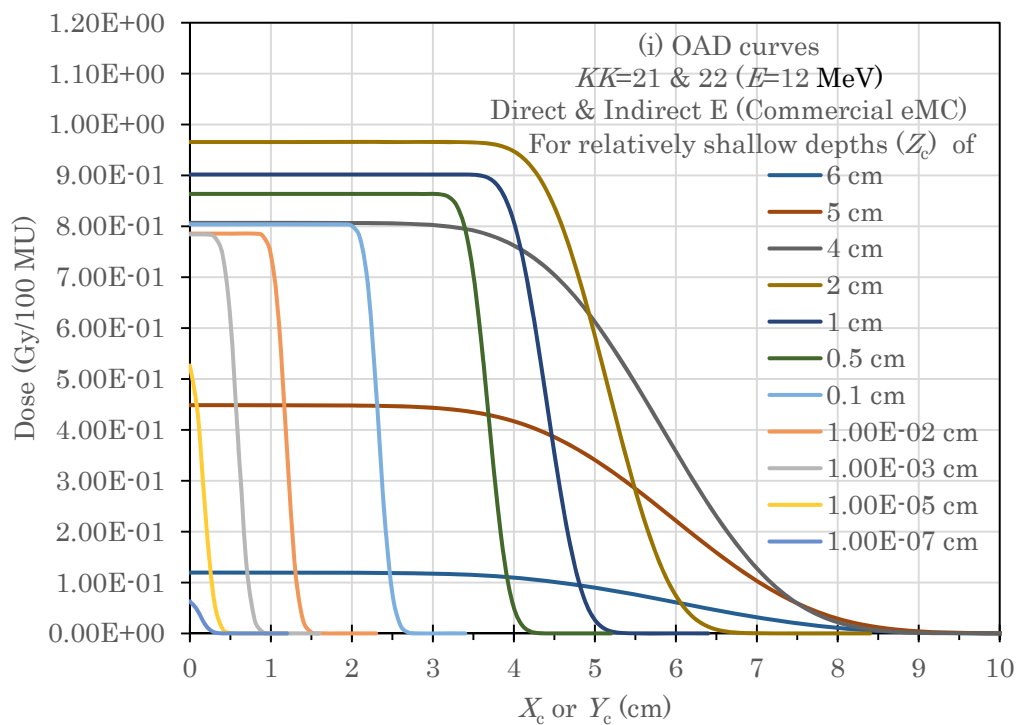


Supp. Fig. 9c

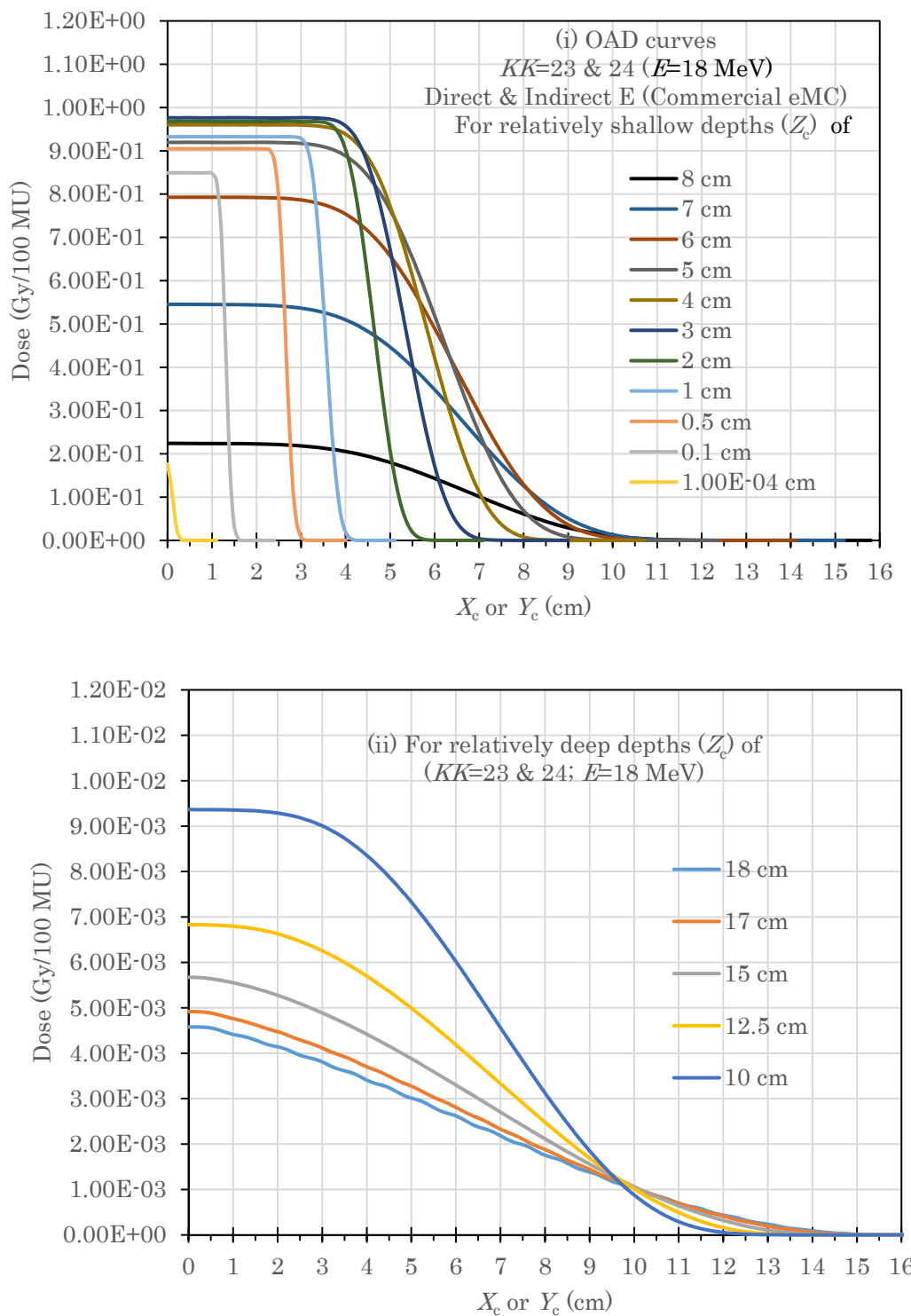
Supp. Fig. 9a-c Each set of diagrams for (a) $KK=13 \text{ & } 14$ (6 MeV), (b) $KK=15 \text{ & } 16$ (12 MeV), or (c) $KK=17 \text{ & } 18$ (18 MeV), produced for *direct & indirect electron beams* on the *standard eMC* using the same way as in Figure 7.



Supp. Fig. 10a



Supp. Fig. 10b



Supp. Fig. 10c

Supp. Fig. 10a-c Each set of diagrams for (a) $KK=19 \text{ & } 20$ (6 MeV), (b) $KK=21 \text{ & } 22$ (12 MeV), or (c) $KK=23 \text{ & } 24$ (18 MeV), produced for *direct & indirect electron beams* on the *commercial eMC* using the same way as in Figure 7.